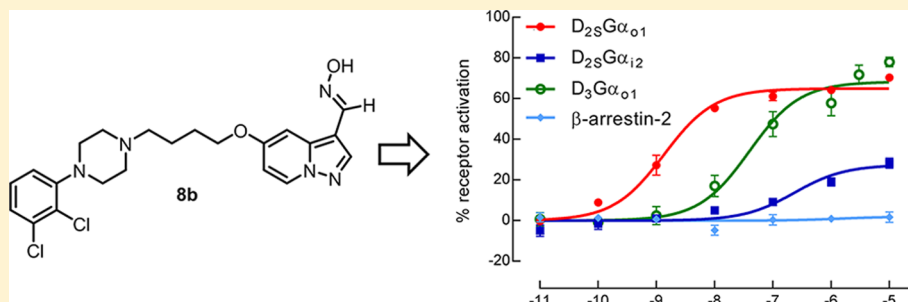


Functionally Selective Dopamine D₂, D₃ Receptor Partial AgonistsDorothee Möller,[†] Ralf C. Kling,[†] Marika Skultety,[†] Kristina Leuner,[‡] Harald Hübner,[†] and Peter Gmeiner^{*,†}[†]Department of Chemistry and Pharmacy, Medicinal Chemistry, and [‡]Department of Chemistry and Pharmacy, Molecular and Clinical Pharmacy, Emil Fischer Center, Friedrich Alexander University, Schuhstrasse 19, 91052 Erlangen, Germany

Supporting Information



ABSTRACT: Dopamine D₂ receptor-promoted activation of Gα_o over Gα_i may increase synaptic plasticity and thereby might improve negative symptoms of schizophrenia. Heterocyclic dopamine surrogates comprising a pyrazolo[1,5-*a*]pyridine moiety were synthesized and investigated for their binding properties when low- to subnanomolar *K_i* values were determined for D_{2L}, D_{2S}, and D₃ receptors. Measurement of [³⁵S]GTPγS incorporation at D_{2S} coexpressed with G-protein subunits indicated significant bias for promotion of Gα_{o1} over Gα_{o2} coupling for several test compounds. Functionally selective D_{2S} activation was most striking for the carbaldoxime **8b** (Gα_{o1}, pEC₅₀ = 8.87, *E*_{max} = 65%; Gα_{o2}, pEC₅₀ = 6.63, *E*_{max} = 27%). In contrast, the investigated 1,4-disubstituted aromatic piperazines (1,4-DAPs) behaved as antagonists for β-arrestin-2 recruitment, implying significant ligand bias for G-protein activation over β-arrestin-2 recruitment at D_{2S} receptors. Ligand efficacy and selectivity between D_{2S} and D₃ activation were strongly influenced by regiochemistry and the nature of functional groups attached to the pyrazolo[1,5-*a*]pyridine moiety.

INTRODUCTION

Schizophrenia is characterized by the coexistence of positive and negative symptoms, cognitive impairment, and a decline in psychosocial functioning.¹ The etiology of schizophrenia is still unknown, but hyper- and hypofunctions in monoamine neurotransmitter systems, especially the mesolimbic and mesocortical dopaminergic pathways, play an important role.² Due to a complex pathophysiology, an adequate treatment of schizophrenia still remains a challenge.^{3,4} Whereas first-generation antipsychotics mainly act via the blockade of dopamine D₂ receptors, second-generation compounds have a broadened receptor-binding profile. This leads to a lower liability to cause extrapyramidal side effects (EPS) and a more efficient treatment of negative symptoms, but goes along with other drawbacks caused by severe side effects including agranulocytosis or obesity.² Third-generation antipsychotics, including aripiprazole (**2a**) and the promising drug candidate *N'*-[*trans*-4-[2-[4-(2,3-dichlorophenyl)-1-piperazinyl]ethyl]-cyclohexyl]-*N,N*-dimethylurea (cariprazine, RGH-188, **2b**), act as partial agonists at D₂ and D₃ receptors, thereby stabilizing the dopaminergic system.^{5–7} Several other attempts to bring dopamine receptor partial agonists to the market [e.g., bifeprunox, 7-[3-(4-[2,3-dimethylphenyl]piperazinyl)propoxy]-2(1*H*)-quinolinone (OPC-4392) and *N*-[(8α)-2-chloro-6-

methylergoline-8-yl]-2,2-dimethylpropanamide (SDZ 208-912)] failed either because of a lack of efficacy or for safety reasons.⁴ The underlying question relating the optimal intrinsic efficacy and ligand selectivity is further complicated by the growing evidence for a phenomenon referred to as functional selectivity or biased agonism.⁸ Functional selectivity explains the capacity of a ligand to preferentially orientate the coupling of a GPCR with a subset of signal transducers, including G-protein-mediated effects and G-protein-independent responses.^{9,10} The possibility to modulate these pathways independently from each other was convincingly demonstrated by applying the angiotensin II receptor as a model system by Lefkowitz and co-workers.^{11,12} Such ligand-induced bias between β-arrestin recruitment and G-protein coupling was also reported for **2a**, **2b**, and structurally related analogues.^{13–15} Interestingly, Masri et al. identified inhibition of β-arrestin-2 recruitment rather than antagonism of G-protein-promoted signaling at D_{2L} and D_{2S} receptors as a common property of clinically effective antipsychotics.¹⁶ Very recently, we could demonstrate that dopaminergics comprising an enyne moiety are able to separate G-protein activation from β-arrestin

Received: March 14, 2014

recruitment and to discriminate between $G\alpha_{o1}$ - and $G\alpha_{i2}$ -mediated signaling at D_{2L} and D_{2S} receptors.¹⁷ Encouraged by these findings on the biased signaling of atypical dopaminergics, we explored novel 1,4-disubstituted aromatic piperazines (1,4-DAPs) of type 1 for their structural determinants of D_2/D_3 subtype selectivity on a functional level, ligand efficacy, and individual ligand controlled activity patterns. $G\alpha_o$ protein triggers neurite outgrowth in several different neuronal cell lines, suggesting that partial agonists that favor the D_2 -promoted activation of $G\alpha_o$ over $G\alpha_i$ may have positive effects on synaptic plasticity^{18–21} and thereby might improve negative symptoms of schizophrenia. Moreover, the D_3 receptor partial agonist **2b** positively affects cognitive deficits in a mouse model treated with phencyclidine.²² Thus, functionally selective promotion of $G\alpha_{o1}$, $G\alpha_{i2}$, and β -arrestin-2-mediated signaling at the D_{2S} receptor, and $G\alpha_{o1}$ activation at the D_3 receptor was investigated. On the basis of recent findings indicating that the nature of the heterocyclic appendage of **2a** derivatives is associated with the ratio of G-protein activation and β -arrestin-promoted signaling,^{23,14} the quinolinone scaffold was bioisosterically replaced. Since an incorporation of the pyrazolo[1,5-*a*]pyridine unit using different attachment points proved to be beneficial for fine-tuning the dopaminergic properties of 1,4-DAPs,^{24–28} we prepared and studied a collection of regioisomeric target compounds of type 1, formally hybridizing the antipsychotic **2a**, the drug candidate **2b**, and our previously described dopaminergics of type 3 (Figure 1).²⁹

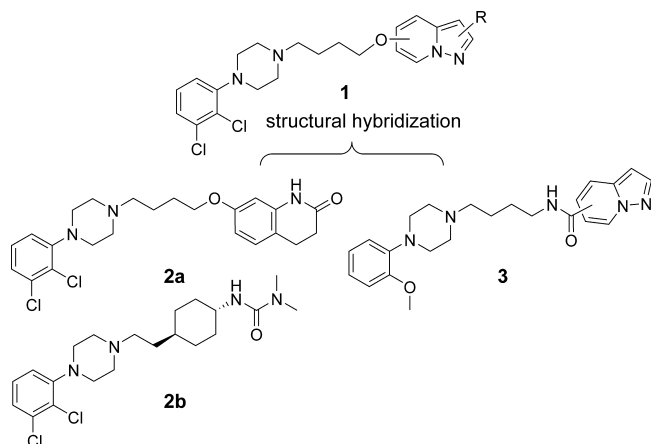


Figure 1. Structural hybridization of **2a**, **2b**, and the dopaminergic azaindoles (**3**).

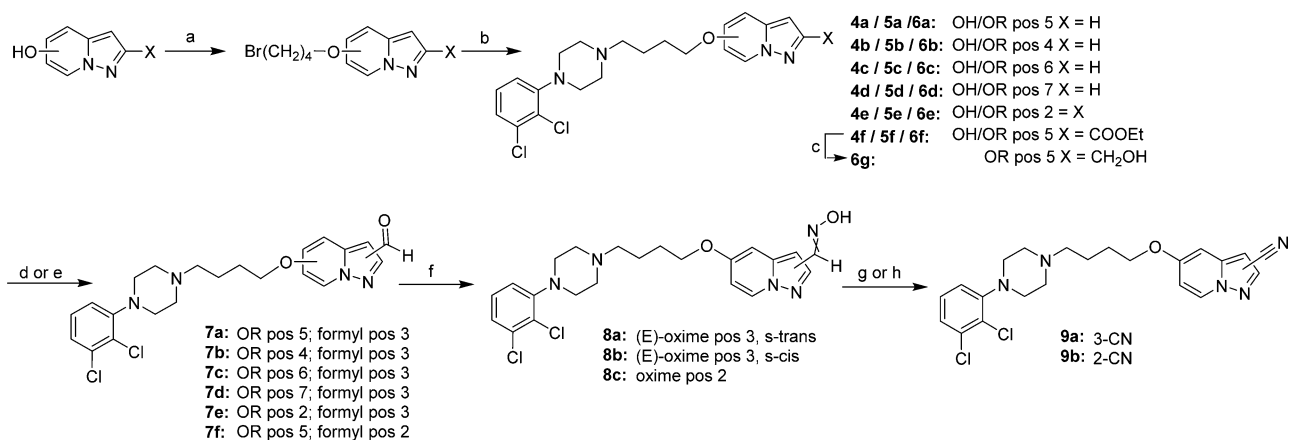
RESULTS AND DISCUSSION

Synthesis. Pyrazolo[1,5-*a*]pyridines were shown to be valuable azaindoles incorporating a hydrogen-bond-accepting nitrogen in position 1.³⁰ The chemically stable heterocyclic system has been proven to be very useful in medicinal chemistry because it is readily accessible by 1,3-dipolar cycloaddition, allowing various functionalizations in any position.³¹ We intended to bioisosterically displace the dihydroquinolinone unit of our lead compound **2a** by the pyrazolo[1,5-*a*]pyridine framework that should be linked to an oxyalkylene spacer via different points of attachment. Introduction of a second H-bond-accepting functional group into the heteroarene moiety mimicking the lactam group of the lead structure **2a** was also envisioned. Starting from 1,4-disubstituted phenylpiperazines (1,4-DAPs), known as priv-

ileged structural surrogates for biogenic amines,^{32,33} we built our synthesis strategy in analogy to previously described routes leading to analogues of **2a** (Scheme 1).^{34–36} Initially, pyrazolo[1,5-*a*]pyridine scaffolds **4a–4e** were prepared in different regioisomeric forms.^{25,29,37–39} For the synthesis of the 5-substituted carboxylate **4f**, we adopted our previously described protocol⁴⁰ involving 1,3-dipolar cycloaddition of dimethylacetylene dicarboxylate and 4-methoxy-*N*-aminopyridinium ions under oxidative conditions, followed by simultaneous ester hydrolysis, decarboxylation, and ether cleavage by hydrobromic acid and subsequent re-esterification (for details, see the Supporting Information).

Alkylation of the phenolic hydroxyl group with 1,4-dibromobutane in analogy to a literature described protocol³⁴ afforded the alkyl bromides **5a–f**, which were subsequently reacted with 1-(2,3-dichlorophenyl)piperazine in the presence of sodium iodide to yield the target compounds **6a–f**. To mimic the carboxamide moiety of the dihydroquinolin-2(1*H*)-one substructure of **2a**, we introduced a formyl group into position 3 of the pyrazolo[1,5-*a*]pyridine ring⁴¹ by a protocol involving the Vilsmeier reaction,⁴² resulting in formation of the test compounds **7a–e**. Because direct formylation of the π -electron-poor position 2 was not possible, the regioisomer **7f** was prepared by reduction of the ethyl ester **6f** and subsequent oxidation of the hydroxymethyl-substituted intermediate **6g** with manganese(IV) oxide. Conversion of the carbaldehydes **7a** and **7f** to the corresponding aldoximes by refluxing with hydroxylamine hydrochloride in ethanol⁴¹ yielded mixtures of *s*-cis and *s*-trans isomers in each case. For the 3-substituted pyrazolo[1,5-*a*]pyridine, the isomers could be separated by column chromatography. Diagnostic NOESY experiments revealed oxime *E*- and *s*-trans configuration for isomer **8a** and a combination of *E* and *s*-cis configuration for isomer **8b**, respectively (Figure 2). Oxime **8c** exists as an inseparable mixture of a major isomer (75%) with *E* and *s*-cis configuration and a minor component (25%) with *s*-trans relationship and an oxime geometry that could not be determined. To study the impact of individual substituents on GPCR binding and activation, the aldoximes **8a,b** and **8c** were converted into the cyano derivatives **9a** and **9b** by employing acetic anhydride and cyanuric chloride/DMF, respectively.^{43–45}

Ligand Binding Experiments. To evaluate the impact of the pyrazolo[1,5-*a*]pyridine-derived lipophilic appendages on receptor binding, radioligand displacement assays were conducted. The resulting affinity and selectivity profiles of the target compounds were compared with those of **2a** and **2b** (Table 1). Binding data were generated by measuring the ability of the test compounds to compete with [³H]spiperone for the cloned human dopamine receptor subtypes D_{2L} , D_{2S} , D_3 , and $D_{4.4}$ stably expressed in Chinese hamster ovary (CHO) cells. D_1 and 5-HT_{2A} receptor affinities were determined utilizing the D_1 -selective radioligand [³H]SCH23390 or [³H]ketanserin and cloned human $D_1/5$ -HT_{2A} receptors transiently expressed in HEK 293 cells. For 5-HT_{1A} and α_1 receptor affinities, competition experiments were performed by employing porcine cortical membranes and the selective radioligands [³H]WAY600135 and [³H]prazosin, respectively. Our initial investigations were directed to the evaluation of the attachment point of the pyrazolo[1,5-*a*]pyridine moiety. Interestingly, all regioisomers of type **6a–6e** displayed K_i values between 2.1 and 64 nM for D_{2L} , D_{2S} , and D_3 receptors, indicating substantial binding affinity. A linkage via position 6 was most favorable, leading to affinities of 4.2, 2.1, and 2.3 nM at D_{2L} , D_{2S} , and D_3

Scheme 1. Synthesis of Dopaminergic Pyrazolo[1,5-*a*]pyridines^a

^aReagents and conditions: (a) 1,4-dibromobutane, K₂CO₃, 60 °C, 8 h (31–85%); (b) (1) NaI, acetonitrile, reflux, 30 min; (2) 1-(2,3-dichlorophenyl)piperazine, Et₃N, 85 °C, 5–16 h (62–84%); (c) LiAlH₄, Et₂O, 0 °C to rt, 3 h (85%); (d) for 7a–7e, POCl₃, DMF, rt, 1 h (40–95%); (e) for 7f, MnO₂, DCM, rt, 14 h (99%); (f) NH₂OH HCl, H₂O/EtOH (1:8), reflux, 2 h (81–82%); (g) for 9a, Ac₂O, reflux, 8 h (72%); (h) for 9b, cyanuric chloride, DMF, rt 7 h (65%).

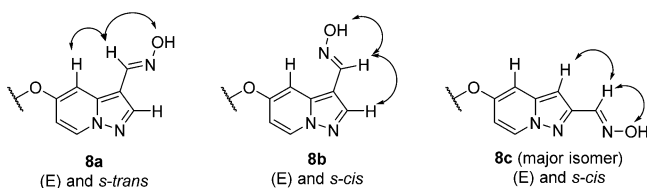


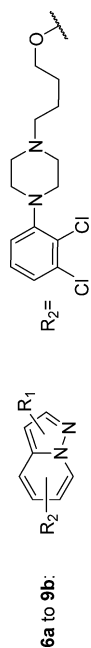
Figure 2. Diagnostic NOESY experiments revealed the exact configuration of aldoximes 8a–8c. Arrows indicate the observed NOE signals in DMSO-*d*₆.

receptors, respectively, for test compound 6c. When the delocalized π -electron system was enlarged by addition of a formyl substituent in position 3 of the heterocyclic ring, an approximately 10-fold increase in D₂ receptor affinity was observed for the 5-alkoxy-substituted azaindole 7a, compared to the nonfunctionalized 5-alkoxy precursor 6a (4.6 and 3.2 nM vs 34 and 39 nM at D_{2L} and D_{2S}, respectively). Likewise, 2–15-fold increases of D₂ affinities were observed for ligands 6f, 6g, and 7f when polar substituents were formally introduced into position 2 of the 5-alkoxy-substituted heteroarene scaffold. The conversion of the carbaldehydes 7a and 7f to the corresponding aldoximes 8a, 8b, and 8c led to low to subnanomolar affinities of 1.8, 0.17, and 3.3 nM at D_{2L}, 1.7, 0.25, and 2.3 nM at D_{2S}, and 2.3, 0.69, and 0.86 nM at D₃ receptors, respectively. Interestingly, the *s*-cis configured aldoxime 8b showed a receptor binding profile similar to those of the lead compounds 2a and 2b, except for a 10–20-fold higher D₄ receptor affinity. Introduction of a cyano group into position 3 of the azaindole ring led to high D₂ affinity: subnanomolar *K_i* values of 0.58 and 0.32 nM were observed for test compound 9a at D_{2L} and D_{2S} receptors, respectively. Interestingly, D₄ and D₃ receptor affinities were in the same low nanomolar range for this 3-substituted cyano derivative (1.5 and 5.7 nM). Only moderate to poor D₁ receptor affinities could be determined for the compound collection. However, *K_i* values in the nanomolar range were observed for the D₄ subtype and 5-HT_{1A}, 5-HT_{2A}, and α_1 receptors.

Functional Experiments. To investigate the impact of the functionalized pyrazolo[1,5-*a*]pyridine moiety on balanced or biased G-protein activation at D_{2S} and D₃ receptors, ligand-

induced nucleotide exchange was determined in cell lines coexpressing receptor and individual G α subunits. Whereas highly selective coupling to G α_{46} has been described for the D₃ subtype, the two isoforms of D₂ (D_{2S} and D_{2L}) are known to couple promiscuously to different G $\alpha_{i/o}$ subunits.^{47–51} However, activation of G α_o has been associated with neurite outgrowth in different neuronal cell lines, thereby offering the possibility to alter interneuronal connections.^{18–21} A reduction of dendritic spines in the hippocampus and prefrontal cortex of schizophrenic patients was found to be associated with cognitive impairment.^{52–54} To better understand differential contributions of distinct signaling pathways of the dopaminergic system, functionally selective ligands are required. To identify such ligands, we performed [³⁵S]GTP γ S incorporation assays with membrane preparations from HEK 293 cells coexpressing D_{2S} receptors and the previously described PTX-insensitive C³⁵²I and C³⁵¹I variants⁵⁵ of G α_{i2} , the most abundant G α_i subunit,^{56,57} and G α_{o1} , the predominant isoform in the central nervous system (CNS), respectively.^{51,58} Pertussis toxin was used in control experiments to exclude interference of endogenously expressed G-proteins in the used HEK cell line (Figure S1, Table S1, Supporting Information). Likewise, ligand-induced activation of D₃ receptors coexpressed with G α_{o1} was evaluated. As indicated in Table 2, the reference agonists quinpirole and dopamine displayed similar potencies for activation of G α_{o1} and G α_{i2} subunits at D_{2S} receptors. However, the endogenous ligand was slightly less effective in G α_{o1} coupling (87% vs 102%). Interestingly, 2a, 2b, and our novel 1,4-DAPs showed substantially higher ligand efficacy for D_{2S}-induced G α_{o1} coupling (*E*_{max} = 25–72%) than for G α_{i2} coupling (*E*_{max} < 3–39%). Functional selectivity for D_{2S}-promoted G α_{o1} activation was most striking for the 5-substituted azaindole-3-carbaldoxime 8b, showing a difference in potency of 2 orders of magnitude and a substantial bias of ligand efficacy (G α_{o1} activation: pEC₅₀ = 8.87, *E*_{max} = 65%; G α_{i2} activation: pEC₅₀ = 6.63, *E*_{max} = 27%) (Figure 3). It is worthy to note that the pEC₅₀ value for 8b induced G α_{o1} activation at the D_{2S} receptor indicated 30-fold higher potency than the lead compound 2a (pEC₅₀ = 7.41), although D_{2S} affinity was in the subnanomolar range for both compounds. Superior and functionally selective D_{2S}G α_{o1} activation was also observed

Table 1. Receptor Binding Data for the Compounds 6a–g, 7a–f, 8a–c, and 9a,b Compared to the Reference Compounds Quinpirole, 2a, and 2b, Employing Human D₁, D_{2L}, D_{2S}, D₃, D_{4,4} and 5-HT_{2A} Receptors and Porcine 5-HT_{1A} and α_1 Receptors



compd	R ₁	R ₂ position	$K_i \pm SD$ (nM) ^a									
			[³ H]SCH23390		[³ H]spiperone		[³ H]WAY100635		[³ H]ketanserin		[³ H]prazosin	
			hD ₁	hD _{2L}	hD _{2S}	hD ₃	hD _{4,4}	p5-HT _{1A}	h5-HT _{2A}	p α_1		
quinpirole			87000 ± 6000	260 ± 38	70 ± 18	15 ± 3.7	8.5 ± 1.4	6300 ± 1100	25000 ± 920 ^b	55000 ± 6200		
2a			310 ± 110	0.54 ± 0.17	0.45 ± 0.05	3.0 ± 0.61	81 ± 14	88 ± 7.1	4.0 ± 1.1	17 ± 0.70		
2b			2100 ± 1200	0.47 ± 0.13	0.41 ± 0.06	0.27 ± 0.07	110 ± 10	0.49 ± 0.13	22 ± 6.0	70 ± 2.5		
6a	H	5	2900 ± 800 ^b	34 ± 12	39 ± 16	7.0 ± 1.3	130 ± 39	110 ± 5.0	390 ± 30 ^b	62 ± 8.0		
6b	H	4	1800 ± 450 ^b	25 ± 3.5	30 ± 6.5	10 ± 2.8	16 ± 0.0	83 ± 11	340 ± 70 ^b	22 ± 1.5		
6c	H	6	1200 ± 340 ^b	4.2 ± 2.2	2.1 ± 0.0	2.3 ± 0.55	4.4 ± 0.95	82 ± 1.0	260 ± 35 ^b	28 ± 7.5		
6d	H	7	580 ± 30 ^b	64 ± 9.5	16 ± 3.0	7.2 ± 2.1	16 ± 3.0	43 ± 16	77 ± 17 ^b	15 ± 0.50		
6e	H	2	1100 ± 190 ^b	9.4 ± 0.60	10 ± 0.65	3.5 ± 0.45	33 ± 2.0	17 ± 2.5	150 ± 0.0 ^b	23 ± 5.0		
6f	2-COOEt	5	150 ± 10	7.4 ± 0.70	6.7 ± 2.4	2.1 ± 0.77	47 ± 18	48 ± 1.0	22 ± 0.0	43 ± 6.2		
6g	2-CH ₂ OH	5	240 ± 20	3.1 ± 2.6	2.3 ± 0.79	1.3 ± 0.54	35 ± 7.4	5.7 ± 1.7	16 ± 1.0	5.1 ± 0.50		
7a	3-CHO	5	970 ± 10	4.6 ± 2.2	3.2 ± 1.1	6.9 ± 3.1	57 ± 13	95 ± 68	240 ± 12	18 ± 0.50		
7b	3-CHO	4	390 ± 5.0 ^b	29 ± 7.0	24 ± 6.0	20 ± 4.5	41 ± 3.5	42 ± 1.0	95 ± 5.5 ^b	20 ± 2.0		
7c	3-CHO	6	570 ± 85 ^b	6.2 ± 0.85	8.1 ± 0.75	2.0 ± 0.05	18 ± 1.0	15 ± 0.0	170 ± 45 ^b	9.7 ± 3.3		
7d	3-CHO	7	1600 ± 250 ^b	51 ± 11	15 ± 0.0	6.4 ± 0.20	78 ± 1.5	31 ± 17	53 ± 15 ^b	15 ± 1.5		
7e	3-CHO	2	590 ± 70 ^b	10 ± 0.55	14 ± 1.5	5.9 ± 0.10	29 ± 6.0	29 ± 1.5	260 ± 130 ^b	11 ± 1.8		
7f	2-CHO	5	180 ± 70	14 ± 8.9	14 ± 4.8	6.0 ± 2.1	89 ± 23	36 ± 1.5	56 ± 6.0	18 ± 2.0		
8a	3-CHNOH (E)-s-trans	5	4300 ± 300	1.8 ± 0.25	1.7 ± 0.10	2.3 ± 0.35	5.3 ± 0.30	21 ± 6.5	7.7 ± 0.50	2.9 ± 0.30		
8b	3-CHNOH (E)-s-cis	5	670 ± 50	0.17 ± 0.05	0.25 ± 0.01	0.69 ± 0.10	6.0 ± 3.5	4.2 ± 1.5	4.0 ± 0.10	6.6 ± 2.7		
8c	2-CHNOH	5	260 ± 75	3.3 ± 1.1	2.3 ± 0.21	0.86 ± 0.12	24 ± 4.7	7.1 ± 1.1	7.9 ± 0.50	8.0 ± 1.2		
9a	3-CN	5	930 ± 280	0.58 ± 0.16	0.32 ± 0.04	1.5 ± 0.51	5.7 ± 1.8	98 ± 13	490 ± 40	13 ± 4.9		
9b	2-CN	5	3500 ± 950	8.9 ± 3.9	6.7 ± 1.6	1.9 ± 0.22	9.3 ± 3.1	16 ± 2.5	81 ± 20	16 ± 4.0		

^aK_i values in nM ± standard error of mean derived from at least two individual experiments each performed in triplicate. ^bData obtained with porcine receptors (pD₁, p5-HT₂).

Table 2. Intrinsic Activities and Potencies of Compounds 2a,b, 6a,c,f,g, 7a,c,f, 8a–c, and 9a,b Determined by [³⁵S]GTPγS Accumulation with Membranes from HEK 293 Cells Transiently Transfected with D₂₅ or D₃ and the PTX Resistant Gα_{o1} or Gα₁₂ G-Protein Subunits

compd	[³⁵ S]GTPγS binding (mean ± SEM) ^a								
	D ₂₅ Gα _{o1}			D ₂₅ Gα ₁₂			D ₃ Gα _{o1}		
	pEC ₅₀	EC ₅₀ (nM)	E _{max} (%) ^b	pEC ₅₀	EC ₅₀ (nM)	E _{max} (%) ^b	pEC ₅₀	EC ₅₀ (nM)	E _{max} (%) ^b
quinpirole	6.21 ± 0.02	610	100 ± 1	5.79 ± 0.02	1600	100 ± 1	8.01 ± 0.03	9.7	100 ± 1
dopamine	6.51 ± 0.09	310	87 ± 4	6.33 ± 0.09	470	102 ± 3	8.03 ± 0.09	9.3	97 ± 4
2a	7.41 ± 0.09	39	67 ± 2	6.80 ± 0.20	160	29 ± 3	7.71 ± 0.17	20	52 ± 3
2b	8.51 ± 0.09	3.1	72 ± 2	6.95 ± 0.13	110	34 ± 2	8.24 ± 0.15	5.8	58 ± 3
6a	6.45 ± 0.09	360	48 ± 2	6.75 ± 0.23	180	22 ± 2	7.18 ± 0.15	66	78 ± 5
6c	8.00 ± 0.09	10	63 ± 2	5.89 ± 0.20	1300	39 ± 4	7.38 ± 0.26	41	41 ± 4
6f	6.13 ± 0.22	740	37 ± 4	6.36 ± 0.24	440	23 ± 3	7.25 ± 0.14	57	67 ± 4
6g	6.59 ± 0.17	260	49 ± 4	6.27 ± 0.19	540	28 ± 3	8.23 ± 0.19	5.9	57 ± 4
7a	6.73 ± 0.11	190	64 ± 3	6.19 ± 0.20	650	27 ± 3	8.72 ± 0.16	1.9	79 ± 5
7c	7.70 ± 0.12	20	64 ± 3	6.47 ± 0.17	340	35 ± 3	6.95 ± 0.21	110	55 ± 5
7f	6.21 ± 0.13	620	25 ± 2	nd	nd	≤3	8.30 ± 0.21	5.0	32 ± 2
8a	8.14 ± 0.09	7.2	53 ± 2	6.56 ± 0.16	270	33 ± 2	7.37 ± 0.13	42	67 ± 4
8b	8.87 ± 0.06	1.3	65 ± 1	6.63 ± 0.18	240	27 ± 2	7.41 ± 0.14	39	68 ± 4
8c	6.21 ± 0.12	610	34 ± 2	nd	nd	≤3	7.82 ± 0.21	15	35 ± 3
9a	7.20 ± 0.11	64	48 ± 2	6.96 ± 0.25	110	18 ± 2	7.91 ± 0.22	12	58 ± 5
9b	5.75 ± 0.10	1800	43 ± 3	7.01 ± 0.27	98	16 ± 2	7.39 ± 0.16	41	60 ± 4

^aData represent mean ± standard error of the mean from the pooled curve of three to eight individual experiments, each performed as triplicates.

^bE_{max} derived from the pooled curve and relative (%) to the maximal effect of quinpirole; nd, not determined.

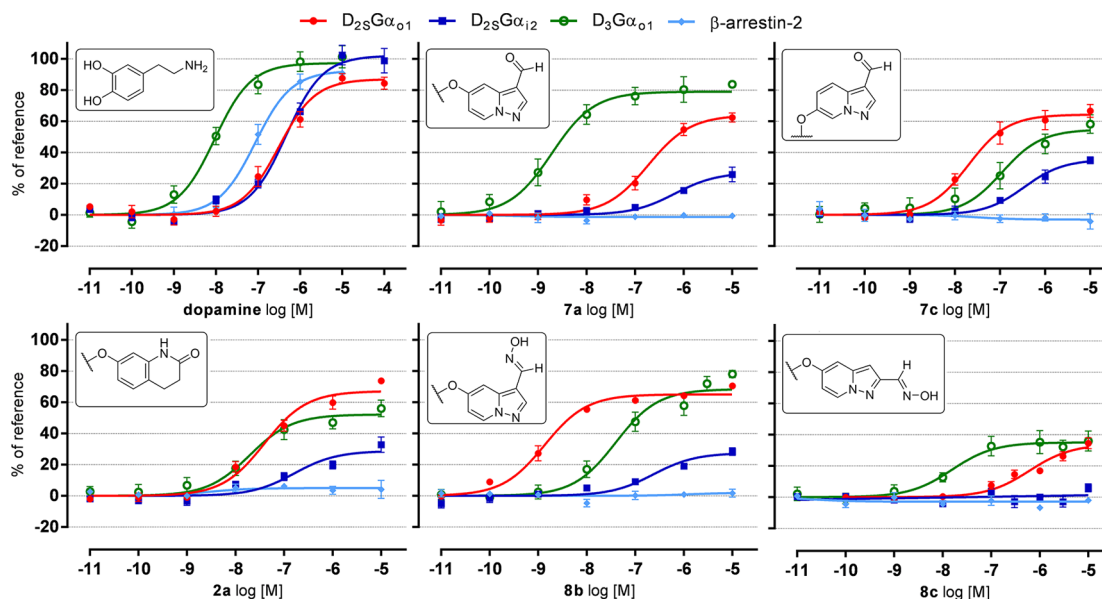


Figure 3. Dose–response curves of the agonist-stimulated [³⁵S]GTPγS binding at D₂₅ and D₃ receptors and β-arrestin-2 recruitment at the D₂₅ receptor. Membranes from HEK 293 cells transiently transfected with D₂₅ or D₃ and the PTX-insensitive G-proteins Gα_{o1} or Gα₁₂ (D₂₅ + Gα_{o1}, red; D₂₅ + Gα₁₂, blue; D₃ + Gα_{o1}, green) or HEK 293-β-arrestin-2 cells transiently transfected with D₂₅-ARMS2-PK2 (light blue) were stimulated with dopamine, 2a, 7a,c, and 8b,c, respectively. Responses were normalized to basal (0%) and the maximum effect of quinpirole (100%).

for the stereoisomeric carbaldoxime 8a with *s*-trans geometry, the unsubstituted 6-alkoxy-azaindole 6c, and its 3-carbaldehyde 7c (pEC₅₀ = 8.14, 8.00, and 7.70, E_{max} = 53, 63, 64%, respectively). Interestingly, lead compound 2b promoted Gα_{o1} coupling with a high potency (pEC₅₀ = 8.51) and the highest intrinsic activity (E_{max} = 72%) of all 1,4-DAPs investigated. Simultaneously, 2b was the most potent compound in D₂₅Gα₁₂ activation (pEC₅₀ = 6.95, E_{max} = 34%).

Regarding D₃ receptor promoted nucleotide exchange, dopamine and quinpirole activated Gα_{o1} coupling with equal potencies and similar efficacies. Compared to the D₂₅Gα_{o1}

activation, potencies were measured to be 50-times higher.^{47,59} Interestingly, our subtle modifications of the pyrazolo[1,5-*a*]pyridine regiochemistry and substitution pattern led to a diverse ligand-controlled receptor activation profile. Whereas the partial agonists 2a and 2b promoted a nearly balanced activation of Gα_{o1} signaling at D₂₅ and D₃ receptors, the 5-alkoxy carbaldehyde 7a preferentially activated D₃ receptors with a pEC₅₀ of 8.72 and a maximal effect of 79% compared to pEC₅₀ of 6.73 and 64% at D₂₅Gα_{o1}, respectively. In contrast, the regioisomeric 6-alkoxy carbaldehyde 7c preferentially activated Gα_{o1} coupling at the D₂₅ receptor. This preference was even

more pronounced for the 3-substituted carbaldoxime **8b**, which promoted $G\alpha_{o1}$ coupling at the D_{25} with a 30-fold selectivity over $G\alpha_{o1}$ coupling at D_3 receptors, although no significant difference in binding affinities for the two receptors was observed. Interestingly, besides the nature of the functional group, the attachment point of the functional group to the pyrazolo[1,5-*a*]pyridine moiety was of particular relevance for ligand efficacy. Whereas a substitution in position 3 of the aromatic heterocycle led to a significant partial agonist effect at D_{25} and D_3 receptors, the regioisomeric functionalization in position 2 reduced ligand efficacy for D_{25} and D_3 coupling to $G\alpha_{o1}$ and even revealed neutral antagonist properties for the 2-substituted carbaldehyde **7f** and the corresponding carbaldoxime **8c** at D_{25} coexpressed with $G\alpha_{i2}$. To further quantify the bias for differential activation of G-proteins elicited by the test compounds, we applied the operational model of agonism first derived by Black and Leff,⁶⁰ as it is one of the methods that allows one to account for differences in potencies and efficacies for different signaling pathways simultaneously.^{61–65} The obtained transduction coefficient $\log(\tau/K_A)$ can be used as an overall measure for the power of an agonist and allows the comparison across different pathways after normalization to a reference agonist [$\Delta\Delta\log(\tau/K_A)$].¹³ As expected, the calculation revealed the aldoxime **8b** as the compound with the highest bias toward $G\alpha_{o1}$ -mediated signaling at the D_{25} receptor [$\Delta\Delta\log(\tau/K_A) = 2.51 \pm 0.28$]. Moreover, this compound showed the strongest preference for D_{25} - over D_3 -promoted activation of $G\alpha_{o1}$ [$\Delta\Delta\log(\tau/K_A) = 3.01 \pm 0.26$] (Table S4, Figure S9, Supporting Information).

Besides G-protein-mediated signaling, β -arrestin recruitment is another important aspect of 7-transmembrane (7-TM) receptor activation.⁹ Moreover, Masri and co-workers identified the inhibition of β -arrestin-2 recruitment at D_2 receptors, rather than antagonism of G-protein activation, as a property shared among clinically effective antipsychotics.¹⁶ Hence, receptor-mediated recruitment of β -arrestin-2 at the D_{25} was investigated by utilizing the DiscoverX PathHunter technology. For this purpose, HEK 293 cells stably expressing a chimeric protein of β -arrestin-2 and an enzyme acceptor (β -galactosidase fragment) were transiently transfected with a D_{25} receptor that was C-terminally tagged with the ARMS2-PK2 donor sequence. Upon stimulation with the test compounds of type **1** and the reference agents, β -arrestin-2 recruitment was determined by measuring the occurring chemiluminescence. For the traditional agonist quinpirole and the endogenous ligand dopamine, full dose–response curves were obtained, whereas the antipsychotic **2a** was not able to induce β -arrestin-2 recruitment. In contrast, the drug candidate **2b** acted as a weak partial agonist with a maximal effect of 11% and a pEC_{50} of 8.46 (data not shown), which is in excellent agreement with the literature.⁶⁶ The most interesting target compounds **6a,c,f,g**, **7a,c,f**, **8a–c**, **9a,b** did not show β -arrestin-2-recruitment at D_{25} , when tested at a concentration up to 10 μM , implying substantial bias for G-protein activation over β -arrestin-2 recruitment at D_{25} receptors.

To prove receptor mediated antagonism, we tested the ability of the test compounds **2a,b**, **7a,f**, and **8b** to inhibit agonist-induced recruitment of β -arrestin-2 at D_{25} receptors (Table 3, Figure S8, Supporting Information). Interestingly, all tested pyrazolo[1,5-*a*]pyridines were able to completely antagonize the agonist-induced β -arrestin-2 recruitment, displaying pIC_{50} values that are similar to the $G\alpha_o$ -promoted potency values obtained from the γS -GTP assay. Whereas the 3-substituted

Table 3. Inhibition of 100 nM Quinpirole-Induced D_{25} -Mediated β -Arrestin-2 Recruitment in HEK 293 Cells for the Reference Compounds Haloperidol, **2a, **2b**, and compounds **7a,f** and **8b****

compd	inhibition of β -arrestin-2 recruitment ^a		
	pIC_{50} ^b	IC ₅₀ (nM)	E_{max} (%) ^{b,c}
haloperidol	9.15 ± 0.05	0.70	0 ± 1
2a	7.95 ± 0.07	11	≤2
2b	8.78 ± 0.08	1.7	13 ± 2
7a	6.44 ± 0.10	360	≤2
7f	7.54 ± 0.11	22	≤1
8b	8.42 ± 0.07	3.8	≤2

^aInhibition of β -arrestin-2 recruitment was measured with the PathHunter assay in HEK 293 cells transiently transfected with D_{25} -ARMS2-PK2 construct coincubated with 100 nM quinpirole and the test compounds. ^bData represent mean ± SEM from the pooled curve of three to eight individual experiments, each performed as duplicates. ^c E_{max} is relative to the maximal effect of 100 nM quinpirole (100%) and the maximal inhibition thereof caused by haloperidol (0%).

aldoxime **8b** was the most potent full inhibitor of β -arrestin-2 recruitment with a pIC_{50} of 8.42, the closely related 3-substituted aldehyde **7a** and its regioisomer **7f** showed pIC_{50} values of 6.44 and 7.54, respectively, corroborating that these atypical dopaminergics show substantial bias between G-protein activation and β -arrestin recruitment. Haloperidol was used as a reference antagonist ($pIC_{50} = 9.15$). Whereas **2a** also behaved as an antagonist, **2b** could not completely attenuate β -arrestin-2 recruitment.

To delineate the physicochemical properties of our compounds, we calculated the lipophilicity (clogP, Table S3, Supporting Information) of the representative pyrazolopyridines **7a**, **8b**, and **9a**, which does not significantly differ from the properties found for the CNS active phenylpiperazines **2a** and **2b**. Moreover, preliminary in vivo studies of the representative compound **7a** showed significant influence on auditory startle response, indicating CNS activity at a concentration of 3 mg/kg, and thus, the ability to cross the blood–brain barrier (Figure S7, Supporting Information). These data are in agreement with our recently published in vivo activity of an analogous pyrazolo[1,5-*a*]pyridine-carboxamide in a MPTP mouse model of Parkinson's disease.⁶⁷

Structure–Affinity/Activity Relationships. The application of 2,3-dichlorophenylpiperazines as atypical dopaminergic pharmacophores leads to a high affinity for D_2 -like receptors for any of the investigated compounds. However, the affinity profile is highly influenced by the heterocyclic headgroup. Whereas most of the pyrazolo[1,5-*a*]pyridines show a small preference for the D_3 over the D_{2L} receptor (1.5–8.9-fold), the enlargement of the delocalized π -electron system by introduction of a formyl-, an oxime-, or a cyano-substituent in position 3 of the heterocycle leads to a preference for D_2 over D_3 receptors for compounds **7a**, **8a,b**, and **9a**. In contrast, high 5-HT_{1A} affinity is observed for the introduction of an H-bond-donating substituent in position 2 of the pyrazolo[1,5-*a*]pyridine moiety (**6g** and **8c**). In any case, introduction of an aldoxime-substituent to the five-membered aromatic ring goes along with an increase in 5-HT_{2A} and α_1 affinity. The investigated compounds behaved as partial agonists for G-protein activation at D_{25} and D_3 receptors and as antagonists for the recruitment of β -arrestin-2 at D_{25} receptors. The intrinsic efficacy for the promotion of G-protein coupling is

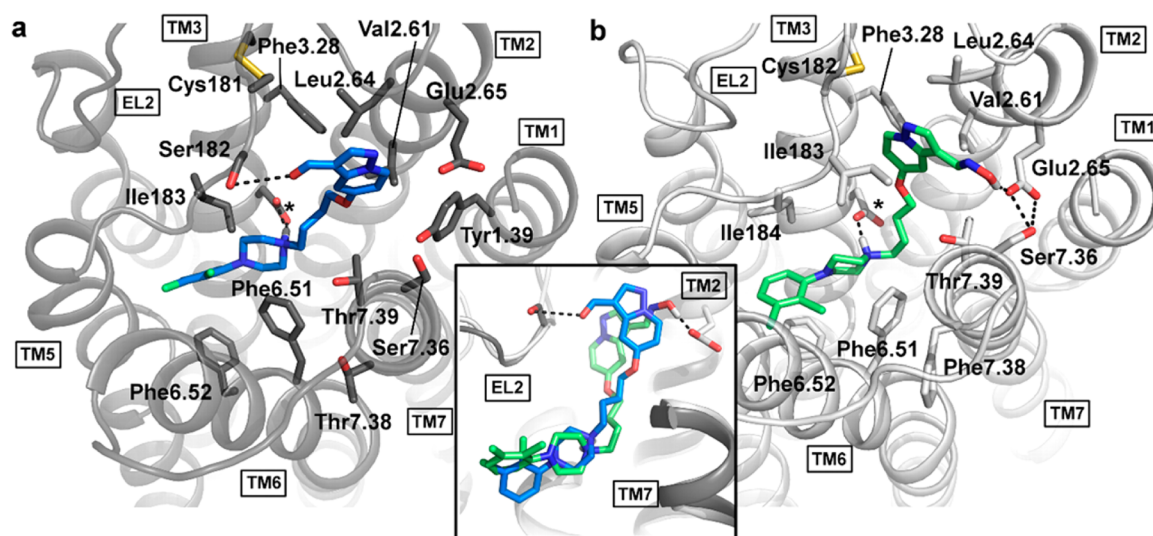


Figure 4. Ligand–receptor interactions for the test compounds **7a** and **8b** bound to D_3 (dark gray ribbons) and D_2 (light gray ribbons), respectively. Amino acids that are expected to stabilize the test compounds have been visualized by dark gray and light gray sticks (* refers to the conserved residue Asp^{3.32}). Compound **7a** within the D_3 receptor is shown by blue sticks (a), whereas compound **8b** within the D_2 receptor is shown by green sticks (b). The inset depicts an alignment indicating conformational differences between the ligands bound to the respective receptor subtype.

related to the substituent of the aromatic heterocycle. Thus, substituents in position 2 lead to a low intrinsic efficacy. H-bond-donating substituents in position 3 such as a carbaldoxime moiety increase the extent of partial agonism observed.

Ligand–Receptor Interactions. To investigate the binding mode of the remarkable test compounds **7a** and **8b** at D_3 and D_2 , respectively, molecular-dynamics-refined docking studies were performed using the crystal structure of the D_3 receptor⁶⁸ and a recently established homology model of D_2 .¹⁷ Therefore, the test compounds **7a** and **8b** were docked into both receptors (Figure S3, Supporting Information). On the basis of a subsequent molecular dynamics (MD) refinement, we selected an energetically favored conformation of **7a** in D_3 and **8b** in D_2 (Figure S4, Supporting Information) and submitted these complexes to simulation runs of 200 and 100 ns for **7a**– D_3 and **8b**– D_2 , respectively, carried out in a pre-equilibrated and hydrated bilayer environment, to allow the test compounds to adapt to their binding sites. We finally performed a cluster analysis on these trajectories and selected representative snapshots of the most highly populated clusters for each ligand–receptor complex (Figure S5, Supporting Information).

Overall, the test compounds **7a** and **8b** occupy virtually identical binding pockets in D_3 and D_2 receptors, respectively, thereby forming interactions to homologous residues of transmembrane helices (TMs) 1–7 and extracellular loops (ELs) 1 and 2 [(Figures 4 and S6 (Supporting Information)]. However, the particular conformations of the test compounds within their binding pockets differ significantly. One of these differences is related to the position of the phenylpiperazine moieties of the test compounds, as the phenylpiperazine part of **7a** is buried around 2 Å deeper in the orthosteric binding site of D_3 than is the case for the analogue **8b** in the D_2 receptor (Figure 4, inset). In addition, compound **8b** showed a flipped conformation of its dichlorophenyl group compared to **7a**. Similar binding modes of closely related 1,4-DAPs have been previously reported.^{13,69,70} In its main conformation, the carbonyl unit of the carbaldoxime **7a** preferentially points toward EL2 of the D_3 receptor (Figure S5, Supporting Information), where it is stabilized by a hydrogen bond to

Ser182 of EL2 [Figures 4a and S5 (Supporting Information)]. As the homologous residue in D_2 is a more lipophilic isoleucine (Ile183), the polar carbaldoxime moiety of **8b** is oriented in the opposite direction, thereby strengthening the interaction of Glu^{2.65} and Ser^{7.36} via hydrogen bonding (Figure 4b). We have observed that the lipophilic appendages of **7a** and **8b** fit into and modify an extended binding site, which was identified earlier to be associated not only with subtype selectivity between D_2 and D_3 ^{26,71} but also with receptor activation and functionally selective signaling.⁷² The predicted binding mode for **7a** and **8b** is in agreement with results from mutational studies employing V2.61F mutants of D_{2L} and D_3 receptors.²⁶ As expected, replacement of the diagnostic residue valine in position 2.61 by a sterically more demanding phenylalanine led to a decrease in receptor affinity (Table S2, Supporting Information) by a factor of 610 and 1230 for **7a** and 46 and 33 for **8b** at D_{2L} and D_3 receptors, respectively. This observation indicates an adoption of an extended binding pocket, which has been described as a general property of 1,4-DAPs.^{26,71} Although the binding modes for the **7a**– D_3 and **8b**– D_2 complexes are similar, some conformations of interacting residues differ significantly between the two subtypes investigated. It is conceivable that subtle modifications at the heterocyclic appendage have a considerable influence on ligand potency and efficacy for different receptor subtypes and signaling pathways, as these would most likely alter the capacity of the compounds to stabilize distinct active-state conformations of the receptors. As the individual transducer protein may alter the ensemble of relevant receptor conformations, comparative studies are required that employ active-state receptors coupled to $G\alpha_i$, $G\alpha_o$, or β -arrestin in order to fully sample the range of conformations stabilized by biased ligands.

CONCLUSIONS

Bioisosteric replacement of the dihydroquinolinone unit of our lead compound **2a** led to a group of atypical dopaminergics comprising a pyrazolo[1,5-*a*]pyridine moiety. To learn more about the structural determinants of D_2/D_3 subtype selectivity on a functional level, ligand efficacy, and individual ligand

controlled activity patterns, we measured ligand binding and [^{35}S]GTP γS incorporation at D_{25} receptors in coexpression with PTX-resistant variants of $\text{G}\alpha_{01}$ or $\text{G}\alpha_{12}$ and D_3 receptors coexpressed with $\text{G}\alpha_{01}$. The investigated 1,4-DAPs showed substantial bias for the promotion of $\text{G}\alpha_{01}$ over $\text{G}\alpha_{12}$ coupling at D_{25} receptors. Because $\text{G}\alpha_o$ protein triggers neurite outgrowth in several different neuronal cell lines,^{18–21} we suggest that partial agonists that favor the D_2 -promoted activation of $\text{G}\alpha_o$ over $\text{G}\alpha_i$ may have beneficial effects on synaptic plasticity and thereby might improve negative symptoms of schizophrenia, as was described for the lead compound aripiprazole previously.^{73–75} Functionally selective D_{25} receptor activation was most striking for the 5-substituted azaindole-3-carbaldoxime **8b**, showing a difference in potency of 2 orders of magnitude and a substantial bias of ligand efficacy. Interestingly, our modifications of the pyrazolo[1,5-*a*]pyridine regiochemistry and substitution led to a diverse ligand controlled receptor activation profile. Whereas the antipsychotic **2a** showed a nearly balanced signaling for $\text{G}\alpha_{01}$ activation at D_{25} and D_3 receptors, the 5-alkoxy-carbaldehyde **7a** preferentially activated D_3 receptors. In contrast, the closely related carbaldoximes **8a,b** and the regioisomeric 6-alkoxy carbaldehyde **7c** preferentially activated $\text{G}\alpha_{01}$ coupling at the D_{25} receptor. Computational studies underlined our findings that subtle modifications of the heteroaromatic pyrazolo[1,5-*a*]pyridine are capable of strongly influencing ligand efficacy and functional selectivity at D_{25} and D_3 receptors. In contrast to their partial agonist activity for G-protein activation, the investigated 1,4-DAPs behaved as neutral antagonists for β -arrestin-2 recruitment, a property that was associated with clinically effective antipsychotics. However, a possible in vivo effect of the investigated 1,4-DAPs will also be influenced by the response to other receptors, as the compounds have a promiscuous receptor affinity profile, including low nanomolar affinity to serotonergic 5-HT $_{1A}$ and 5-HT $_{2A}$ and α_1 receptors.

EXPERIMENTAL SECTION

Chemistry. Reagents and dry solvents were of commercial grade and used as purchased. Except for 1,3-dipolar cycloadditions and ester/ether hydrolysis, all reactions were carried out under nitrogen atmosphere. MS was run on a Bruker Esquire 2000 by APC or ES ionization. HR-EIMS was run on a JEOL JMS-GC mate II with a solid inlet and EI (70 eV) using peak-matching ($M/\Delta M > 5000$). NMR spectra were obtained on a Bruker Avance 360 or a Bruker Avance 600 spectrometer at ambient temperature. All ^1H and ^{13}C chemical shifts are reported in ppm (δ) relative to TMS in the solvents indicated (J in hertz). Melting points were determined with a MEL-TEMP II apparatus (Laboratory Devices) in open capillaries and are given uncorrected. IR spectra were performed on a JASCO FT/IR 410 or a JASCO FT/IR 4100 spectrometer. Purification by column chromatography was performed using silica gel 60. TLC analyses were performed using Merck 60 F254 aluminum sheets and analyzed with UV light (254 nm). Analytical HPLC was performed on Agilent 1100 HPLC systems employing a VWL detector or on Agilent 1200 HPLC systems using a DAD detector. As column, a ZORBAX ECLIPSE XDB-C8 (4.6 mm \times 150 mm, 5 μm) was used. HPLC purity was measured using the following binary solvent system: 10% CH_3OH in 0.1% aqueous formic acid for 3 min, from 10% to 100% CH_3OH in 15 min, and 100% CH_3OH for 6 min (flow rate 0.5 mL/min, $\lambda = 254$ nm). The purity of all test compounds and key intermediates was determined to be >95%. C, H, N elementary analyses were performed at the Chair of Organic Chemistry, Friedrich Alexander University Erlangen-Nuremberg.

5-(4-Bromobutoxy)pyrazolo[1,5-*a*]pyridine (5a). To a suspension of **4a** (1.19 g, 8.88 mmol) and K_2CO_3 (1.23 g, 8.89 mmol) in DMF (44.1 mL) was added 1,4-dibromobutane (3.18 mL, 26.7 mmol) dropwise. After stirring at 60 $^\circ\text{C}$ for 8 h, H_2O was added and the

aqueous layer was extracted with ethyl acetate. The combined organic layers were dried over Na_2SO_4 and evaporated. The crude product was purified by flash chromatography (hexane/EtOAc 2:3) to yield **5a** as an orange oil (1.69 g, 71%). IR (NaCl): 3097, 2945, 2874, 1648, 1537, 1290, 1227, 1040, 746 cm^{-1} . ^1H NMR (CDCl_3 , 360 MHz): δ 1.95–2.02 (m, 2 H), 2.04–2.12 (m, 2 H), 3.50 (t, $J = 6.5$ Hz, 2 H), 4.02 (t, $J = 6.5$ Hz, 2 H), 6.30–6.31 (m, 1 H), 6.43 (dd, $J = 7.8, 2.6$ Hz, 1 H), 6.72 (d, $J = 2.6$ Hz, 1 H), 7.85 (d, $J = 2.1$ Hz, 1 H), 8.28 (d, $J = 7.8$ Hz, 1 H). ^{13}C NMR (CDCl_3 , 360 MHz): δ 27.6, 29.4, 33.2, 67.2, 95.4, 95.5, 106.6, 129.4, 141.0, 142.8, 155.5. HPLC: $t_R = 22.5$ min, purity 96%. APCI-MS: m/z 268 [$\text{M}^+ - 1$], 270 [$\text{M}^+ + 1$]. Anal. Calcd (%) for $\text{C}_{11}\text{H}_{13}\text{N}_2\text{OBr}$: C 49.09, H 4.87, N 10.41. Found: C 48.94, H 4.78, N 10.23.

6-(4-Bromobutoxy)pyrazolo[1,5-*a*]pyridine (5c). Compound **5c** was prepared according to the protocol of **5a** using a suspension of **4c** (110 mg, 0.82 mmol) and anhydrous K_2CO_3 (120 mg, 0.87 mmol) in DMF (4.1 mL) and 1,4-dibromobutane (0.29 mL, 2.46 mmol). The crude compound was purified by flash chromatography (hexane/EtOAc 1:1) to yield **5c** as off-white solid (153 mg, 70%). Mp: 55 $^\circ\text{C}$. IR: 3105, 2943, 2873, 1642, 1525, 1291, 1239, 1199, 1025, 756 cm^{-1} . ^1H NMR (CDCl_3 , 360 MHz): δ 1.96–2.01 (m, 2 H), 2.07–2.11 (m, 2 H), 3.50 (t, $J = 6.6$ Hz, 2 H), 3.99 (t, $J = 5.9$ Hz, 2 H), 6.45 (d, $J = 2.1$ Hz, 1 H), 6.91 (dd, $J = 9.5, 2.2$ Hz, 1 H), 7.41 (d, $J = 9.5$ Hz, 1 H), 7.84 (d, $J = 2.2$ Hz, 1 H), 8.05–8.06 (m, 1 H). ^{13}C NMR (CDCl_3 , 360 MHz): δ 27.8, 29.4, 33.3, 68.0, 96.8, 111.8, 117.9, 119.0, 136.5, 140.8, 148.2. HPLC: $t_R = 22.8$ min, purity 100%. HR-EIMS: calcd 268.0211; found 268.0213. Anal. Calcd (%) for $\text{C}_{11}\text{H}_{13}\text{N}_2\text{OBr}$: C 49.09, H 4.87, N 10.41. Found: C 49.26, H 4.84, N 10.44.

Ethyl 5-(4-Bromobutoxy)pyrazolo[1,5-*a*]pyridine-2-carboxylate (5f). Compound **5f** was prepared according to the protocol of **5a** using a suspension of **4f** (1.36 g, 6.58 mmol) and K_2CO_3 (910 mg, 6.58 mmol) in DMF (34.0 mL) and 1,4-dibromobutane (2.36 mL, 19.8 mmol). The crude compound was purified by flash chromatography (hexane/EtOAc 3:1) to yield **5f** as rose solid (1.41 g, 63%). Mp: 102 $^\circ\text{C}$. IR (NaCl): 3123, 3079, 2988, 2958, 1717, 1644, 1538, 1469, 1403, 1392, 1245, 1200, 1105, 858 cm^{-1} . ^1H NMR (CDCl_3 , 600 MHz): δ 1.44 (t, $J = 7.2$ Hz, 3 H), 1.97–2.03 (m, 2 H), 2.06–2.11 (m, 2 H), 3.50 (t, $J = 6.5$ Hz, 2 H), 4.03 (t, $J = 5.9$ Hz, 2 H), 4.46 (q, $J = 7.1$ Hz, 2 H), 6.57 (dd, $J = 7.7, 2.6$ Hz, 1 H), 6.75 (d, $J = 2.5$ Hz, 1 H), 6.87 (s, 1 H), 8.34 (d, $J = 7.6$ Hz, 1 H). ^{13}C NMR (CDCl_3 , 360 MHz): δ 14.4, 27.5, 29.3, 33.0, 61.3, 67.4, 95.9, 98.7, 109.4, 129.7, 141.8, 145.9, 162.8. HPLC: $t_R = 20.7$ min, purity 97%. HR-EIMS: calcd 340.0423; found 340.0422.

5-[4-[4-(2,3-Dichlorophenyl)piperazin-1-yl]butoxy]pyrazolo[1,5-*a*]pyridine (6a). A solution of **5a** (456 mg, 1.69 mmol) and NaI (381 mg, 2.54 mmol) in acetonitrile (7.6 mL) was refluxed for 30 min. After cooling down, a solution of 1-(2,3-dichlorophenyl)piperazine (430 mg, 1.86 mmol) in triethylamine (0.26 mL, 1.86 mmol) was added and the resulting suspension was stirred at 85 $^\circ\text{C}$ for another 5 h. Then saturated NaHCO_3 solution was added and the aqueous layer was extracted with CH_2Cl_2 . The combined organic layers were dried over Na_2SO_4 and evaporated. The residue was purified by flash chromatography (CH_2Cl_2 + 2% MeOH) to yield **6a** as off-white solid (545 mg, 75%). Mp: 105 $^\circ\text{C}$. IR (NaCl): 2944, 2817, 1647, 1578, 1290, 1227, 1190, 1044, 774 cm^{-1} . ^1H NMR (CDCl_3 , 600 MHz): δ 1.69–1.77 (m, 2 H), 1.84–1.92 (m, 2 H), 2.50 (t, $J = 7.2$ Hz, 2 H), 2.65–2.67 (m, 4 H), 3.06–3.09 (m, 4 H), 4.02 (t, $J = 6.5$ Hz, 2 H), 6.29–6.30 (m, 1 H), 6.44 (dd, $J = 7.6, 2.6$ Hz, 1 H), 6.73 (d, $J = 2.6$ Hz, 1 H), 6.95 (dd, $J = 6.7, 2.9$ Hz, 1 H), 7.13–7.15 (m, 2 H), 7.85 (d, $J = 2.1$ Hz, 1 H), 8.28 (d, $J = 7.6$ Hz, 1 H). ^{13}C NMR (CDCl_3 , 360 MHz): δ 23.4, 27.0, 51.4, 53.3, 58.1, 68.0, 95.3, 95.4, 106.7, 118.6, 124.6, 127.4, 127.5, 129.3, 134.0, 141.1, 142.7, 151.3, 155.7. HPLC: $t_R = 17.1$ min, purity 95%. APCI-MS: m/z 419 [M^+], 421 [$\text{M}^+ + 2$]. Anal. Calcd (%) for $\text{C}_{21}\text{H}_{24}\text{N}_4\text{OCl}_2$: C 60.15, H 5.77, N 13.36. Found: C 59.79, H 5.81, N 13.14.

6-[4-[4-(2,3-Dichlorophenyl)piperazin-1-yl]butoxy]pyrazolo[1,5-*a*]pyridine (6c). Compound **6c** was prepared according to the protocol of **6a** using a solution of **5c** (40.0 mg, 0.15 mmol) and NaI (33.5 mg, 0.22 mmol) in acetonitrile (0.9 mL) as well as a solution of 1-(2,3-dichlorophenyl)piperazine (37.8 mg, 0.16 mmol) in triethyl-

amine (0.05 mL). After purification by flash chromatography (CH_2Cl_2 + 2% MeOH) **6c** was obtained as an off-white solid (43.0 mg, 69%). Mp: 97 °C. IR (NaCl): 3106, 2944, 2811, 1647, 1578, 1291, 1240, 1199, 1043, 781 cm^{-1} . ^1H NMR (CDCl_3 , 360 MHz): δ 1.72–1.81 (m, 2 H), 1.85–1.93 (m, 2 H), 2.54 (t, J = 7.6 Hz, 2 H), 2.68–2.73 (m, 4 H), 3.10–3.12 (m, 4 H), 4.00 (t, J = 6.3 Hz, 2 H), 6.44–6.45 (m, 1 H), 6.92 (dd, J = 9.6, 2.2 Hz, 1 H), 6.96 (dd, J = 6.9, 2.6 Hz, 1 H), 7.14–7.16 (m, 2 H), 7.41 (d, J = 9.6 Hz, 1 H), 7.84 (d, J = 2.2 Hz, 1 H), 8.07–8.08 (m, 1 H). ^{13}C NMR (CDCl_3 , 360 MHz): δ 23.2, 27.1, 51.1, 53.3, 58.1, 68.7, 96.7, 111.8, 117.8, 118.7, 119.1, 124.7, 127.5, 127.6, 134.1, 136.4, 140.8, 148.3, 151.2. HPLC: t_{R} = 19.0 min, purity 99%. APCI-MS: m/z 419 [M^+], 421 [M^+ + 2]. Anal. Calcd (%) for $\text{C}_{21}\text{H}_{24}\text{N}_4\text{OCl}_2 \cdot 0.6\text{H}_2\text{O}$: C 58.64, H 5.91, N 13.03. Found: C 58.86, H 5.81, N 12.78.

Ethyl 5-[4-[4-(2,3-Dichlorophenyl)piperazin-1-yl]butoxy]pyrazolo[1,5-a]pyridine-2-carboxylate (6f). Compound **6f** was prepared according to the protocol of **6a** using a solution of **5f** (504 mg, 1.48 mmol) and NaI (332 mg, 2.21 mmol) in acetonitrile (12.0 mL) as well as a solution of 1-(2,3-dichlorophenyl)piperazine (375 mg, 1.62 mmol) and triethylamine (0.23 mL, 1.66 mmol) in acetonitrile (6.0 mL). The crude compound was purified by flash chromatography (CH_2Cl_2 + 1% MeOH) to afford **6f** as white solid (297 mg, 41%). Mp: 144 °C. IR (NaCl): 3062, 2945, 2878, 2818, 1725, 1649, 1577, 1540, 1495, 1448, 1240, 1221, 1139, 963 cm^{-1} . ^1H NMR (CDCl_3 , 600 MHz): δ 1.44 (t, J = 7.1 Hz, 3 H), 1.71–1.78 (m, 2 H), 1.86–1.89 (m, 2 H), 2.50 (t, J = 7.6 Hz, 2 H), 2.63–2.71 (m, 4 H), 3.05–3.13 (m, 4 H), 4.04 (t, J = 6.3 Hz, 2 H), 4.47 (q, J = 7.1 Hz, 2 H), 6.57 (dd, J = 7.6, 2.6 Hz, 1 H), 6.76 (d, J = 2.4 Hz, 1 H), 6.85 (d, J = 0.8 Hz, 1 H), 6.95 (dd, J = 7.3, 2.4 Hz, 1 H), 7.13 (t, J = 7.7 Hz, 1 H), 7.16 (dd, J = 7.6, 2.0 Hz, 1 H), 8.34 (ddd, J = 7.3, 0.6, 0.6 Hz, 1 H). ^{13}C NMR (CDCl_3 , 360 MHz): δ 14.4, 23.4, 26.9, 51.3, 53.3, 58.0, 61.3, 68.2, 95.9, 98.6, 109.5, 118.6, 124.6, 127.4, 127.5, 129.6, 134.0, 141.9, 145.9, 151.3, 156.0, 162.9. HPLC: t_{R} = 17.0 min, purity 98%. HR-EIMS: calcd 490.1539; found 490.1535.

(5-[4-[4-(2,3-Dichlorophenyl)piperazin-1-yl]butoxy]pyrazolo[1,5-a]pyridin-2-yl)methanol (6g). To an ice-cooled solution of **6f** (56.2 mg, 0.12 mmol) in Et_2O (10.0 mL) was added a 4 M solution of LiAlH_4 in Et_2O (29 μL , 0.12 mmol). After stirring at 0 °C for 1 h the cooling was removed and the solution was stirred at room temperature for 2 h. Then saturated NaHCO_3 solution (30 mL) was added, the organic layer was separated, and the aqueous layer was extracted with CH_2Cl_2 . The combined organic layers were dried over MgSO_4 and concentrated. The residue was purified by flash chromatography (CH_2Cl_2 + 1% MeOH) to afford **6g** as a rose solid (43.8 mg, 85%). Mp: 116 °C. IR (NaCl): 3298, 2926, 2823, 1646, 1577, 1541, 1228, 1421, 1241, 1203, 1044 cm^{-1} . ^1H NMR (CDCl_3 , 600 MHz): δ 1.72–1.80 (m, 2 H), 1.86–1.92 (m, 2 H), 1.92–2.06 (bs, 1H, OH) 2.53 (t, J = 6.7 Hz, 2 H), 2.65–2.75 (m, 4 H), 3.07–3.14 (m, 4 H), 4.02 (t, J = 6.3 Hz, 2 H), 4.85 (s, 2 H), 6.28 (s, 1 H), 6.43 (dd, J = 7.6 Hz, 2.7 Hz, 1 H), 6.67 (d, J = 2.5 Hz, 1 H), 6.96 (dd, J = 7.4, 2.1 Hz, 1 H), 7.14–7.21 (m, 2 H), 8.21 (ddd, J = 7.6, 0.5, 0.5 Hz, 1 H); signal for free OH not detected. ^{13}C NMR (CDCl_3 , 600 MHz): δ 23.3, 26.9, 51.3, 53.3, 58.1, 59.4, 68.0, 93.6, 95, 106.7, 118.6, 124.6, 127.4, 127.5, 129.2, 134.1, 142.2, 151.3, 155.7, 155.9. HPLC: t_{R} = 15.9 min, purity 95%. HR-EIMS: calcd 448.1433; found 448.1434.

5-[4-[4-(2,3-Dichlorophenyl)piperazin-1-yl]butoxy]pyrazolo[1,5-a]pyridine-3-carbaldehyde (7a). To a solution of **6a** (360 mg, 0.86 mmol) in DMF (2.75 mL) was added POCl_3 (0.25 mL, 2.66 mmol). After stirring at room temperature for 1 h, the mixture was diluted with H_2O under ice cooling and alkalinized by addition of 5 M NaOH. After extraction with CHCl_3 , the combined organic layers were dried over Na_2SO_4 and evaporated. The residue was purified by flash chromatography (CH_2Cl_2 + 2% MeOH) to yield **7a** as off-white solid (361 mg, 94%). Mp: 107 °C. IR (NaCl): 2946, 2818, 1663, 1633, 1577, 1527, 1275, 1241, 1194, 1044, 774 cm^{-1} . ^1H NMR (CDCl_3 , 600 MHz): δ 1.70–1.78 (m, 2 H), 1.88–1.96 (m, 2 H), 2.51 (t, J = 7.6 Hz, 2 H), 2.64–2.68 (m, 4 H), 3.07–3.09 (m, 4 H), 4.16 (t, J = 6.5 Hz, 2 H), 6.71 (dd, J = 7.6, 2.6 Hz, 1 H), 6.96 (dd, J = 6.5, 3.0 Hz, 1 H), 7.14–7.15 (m, 2 H), 7.58 (d, J = 2.6 Hz, 1 H), 8.26 (s, 1 H), 9.95 (s, 1 H). ^{13}C NMR (CDCl_3 , 360 MHz): δ 23.3, 26.9, 51.4, 53.3, 58.0, 68.9,

97.7, 109.6, 113.2, 118.6, 124.6, 127.4, 127.5, 130.1, 134.0, 141.6, 147.5, 151.3, 160.6, 183.2. HPLC: t_{R} = 17.1 min, purity 98%. APCI-MS: m/z 446 [M^+ - 1], 448 [M^+ + 1]. Anal. Calcd (%) for $\text{C}_{22}\text{H}_{24}\text{N}_4\text{O}_2\text{Cl}_2 \cdot 0.3\text{H}_2\text{O}$: C 58.36, H 5.48, N 12.37. Found: C 58.34, H 5.43, N 12.27.

6-[4-[4-(2,3-Dichlorophenyl)piperazin-1-yl]butoxy]pyrazolo[1,5-a]pyridine-3-carbaldehyde (7c). Compound **7c** was prepared according to the protocol of **7a** using a solution of **6c** (60.0 mg, 0.14 mmol) in DMF (0.46 mL) as well as POCl_3 (0.04 mL, 0.44 mmol). The crude compound was purified by flash chromatography (CH_2Cl_2 + 2% MeOH) to give **7c** as off-white solid (40.0 mg, 63%). Mp: 99 °C. IR (NaCl): 3096, 2946, 2818, 1663, 1578, 1519, 1278, 1242, 1185, 1044, 780 cm^{-1} . ^1H NMR (CDCl_3 , 360 MHz): δ 1.71–1.79 (m, 2 H), 1.88–1.95 (m, 2 H), 2.51 (t, J = 7.6 Hz, 2 H), 2.64–2.70 (m, 4 H), 3.06–3.11 (m, 4 H), 4.05 (t, J = 6.4 Hz, 2 H), 6.96 (dd, J = 6.6, 3.0 Hz, 1 H), 7.14–7.15 (m, 2 H), 7.30 (dd, J = 9.7, 2.2 Hz, 1 H), 8.16–8.18 (m, 2 H), 8.29 (s, 1 H), 9.98 (s, 1 H). ^{13}C NMR (CDCl_3 , 360 MHz): δ 23.3, 27.0, 51.4, 53.4, 58.0, 69.1, 112.8, 113.9, 118.7, 119.1, 123.7, 124.6, 127.5, 127.6, 134.1, 135.5, 146.2, 150.6, 151.3, 183.1. HPLC: t_{R} = 17.0 min, purity 95%. APCI-MS: m/z 447 [M^+], 449 [M^+ + 2]. Anal. Calcd (%) for $\text{C}_{22}\text{H}_{24}\text{N}_4\text{O}_2\text{Cl}_2$: C 59.07, H 5.41, N 12.52. Found: C 58.68, H 5.43, N 12.16.

5-[4-[4-(2,3-Dichlorophenyl)piperazin-1-yl]butoxy]pyrazolo[1,5-a]pyridine-2-carbaldehyde (7f). To a solution of **6g** (56.8 mg, 0.126 mmol) in CH_2Cl_2 (5.0 mL) was added MnO_2 (110 mg, 1.26 mmol). After stirring at room temperature for 14 h, the remaining MnO_2 was removed by filtration over Celite and the solvent was evaporated to yield **7f** as white solid (55.9 mg, 99%). Mp: 121 °C. IR (NaCl): 3093, 2946, 2876, 2816, 2359, 2248, 1699, 1648, 1577, 1540, 1493, 1447, 1421, 1257, 1207, 1138, 1044, 1016 cm^{-1} . ^1H NMR (CDCl_3 , 600 MHz): δ 1.71–1.80 (m, 2 H), 1.87–1.94 (m, 2 H), 2.52 (t, J = 7.3 Hz, 2 H), 2.64–2.72 (m, 4 H), 3.04–3.13 (m, 4 H), 4.05 (t, J = 6.4 Hz, 2 H), 6.64 (dd, J = 7.6, 2.6 Hz, 1 H), 6.79 (d, J = 2.6 Hz, 1 H), 6.82 (d, J = 0.8 Hz, 1 H), 6.96 (dd, J = 7.4, 2.3 Hz, 1 H), 7.13–7.18 (m, 2 H), 8.31 (ddd, J = 7.6, 0.8, 0.8 Hz, 1 H), 10.16 (s, 1 H). ^{13}C NMR (CDCl_3 , 360 MHz): δ 23.4, 26.9, 51.4, 53.3, 58.0, 68.3, 95.5, 96.3, 110.3, 118.6, 124.6, 127.4, 127.5, 129.6, 134.1, 142.3, 151.3, 152.5, 156.2, 187.7. HPLC: t_{R} = 16.6 min, purity 97%. HR-EIMS: calcd 446.1276; found 446.1276.

(E)-5-[4-[4-(2,3-Dichlorophenyl)piperazin-1-yl]butoxy]pyrazolo[1,5-a]pyridine-3-carbaldehyde Oxime (8a,b). A solution of hydroxylamine hydrochloride (18.0 mg, 0.26 mmol) in water (0.74 mL) and 2 M NaOH (0.07 mL, 0.14 mmol) was adjusted to pH 5.0 by the addition of 2 M HCl and cooled to 0 °C. Subsequently, a solution of **7a** (57.8 mg, 0.13 mmol) in ethanol (6.45 mL) was added and the mixture was refluxed for 2 h. After cooling, saturated NaHCO_3 solution was added and the aqueous layer was extracted with dichloromethane. The combined organic layers were dried over Na_2SO_4 and evaporated. Purification of the residue by flash chromatography ($\text{CH}_2\text{Cl}_2/\text{MeOH}$ 2%) yielded the isomers **8a** (*s*-trans, 25.0 mg, 42%) and **8b** (*s*-cis, 23.5 mg, 39%) as white solids. Isomer **8a**: Mp: 189 °C. IR (KBr): 3446, 3078, 2956, 2831, 1647, 1578, 1535, 1267, 1244, 1038, 789 cm^{-1} . ^1H NMR ($\text{DMSO}-d_6$, 360 MHz): δ 1.60–1.68 (m, 2 H), 1.79–1.86 (m, 2 H), 2.44 (t, J = 7.6 Hz, 2 H), 2.52–2.60 (m, 4 H), 2.97–3.00 (m, 4 H), 4.09 (t, J = 6.4 Hz, 2 H), 6.68 (dd, J = 7.6, 2.6 Hz, 1 H), 7.11 (dd, J = 6.5, 3.0 Hz, 1 H), 7.26–7.30 (m, 3 H), 8.08 (s, 1 H), 8.29 (s, 1 H), 8.58 (d, J = 7.6 Hz, 1 H), 10.63 (s, 1 H). ^{13}C NMR ($\text{DMSO}-d_6$, 360 MHz): δ 23.2, 26.9, 51.5, 53.3, 57.8, 68.6, 97.0, 104.4, 108.0, 120.1, 124.9, 126.6, 129.0, 130.9, 133.2, 138.6, 142.5, 143.1, 151.6, 157.5. HPLC: t_{R} = 16.8 min, purity 99%. APCI-MS: m/z 462 [M^+], 464 [M^+ + 2]. Anal. Calcd (%) for $\text{C}_{22}\text{H}_{25}\text{N}_5\text{O}_2\text{Cl}_2 \cdot 0.4\text{H}_2\text{O}$: C 56.27, H 5.54, N 14.91. Found: C 56.48, H 5.47, N 14.69. Isomer **8b**: Mp: 165 °C. IR (NaCl): 3425, 2846, 1684, 1649, 1542, 1204, 1051, 764 cm^{-1} . ^1H NMR ($\text{DMSO}-d_6$, 360 MHz): δ 1.60–1.68 (m, 2 H), 1.79–1.86 (m, 2 H), 2.43 (t, J = 7.6 Hz, 2 H), 2.52–2.58 (m, 4 H), 2.97–3.00 (m, 4 H), 4.14 (t, J = 6.3 Hz, 2 H), 6.68 (dd, J = 7.6, 2.6 Hz, 1 H), 7.11 (dd, J = 6.5, 3.0 Hz, 1 H), 7.27–7.30 (m, 2 H), 7.45 (d, J = 2.6 Hz, 1 H), 7.75 (s, 1 H), 8.56–8.59 (m, 2 H), 11.06 (s, 1 H). ^{13}C NMR ($\text{DMSO}-d_6$, 360 MHz): δ 23.2, 26.8, 51.5, 53.3, 57.7, 68.8, 95.6, 103.1, 108.0, 120.0, 124.8,

126.5, 128.9, 130.6, 133.1, 137.0, 140.5, 145.6, 151.7, 157.4. HR-EIMS: calcd 461.1385; found 461.1385. HPLC: t_R = 18.1 min, purity 99%. Anal. Calcd (%) for $C_{22}H_{25}N_5O_2Cl_2 \cdot 0.5H_2O$: C 56.06, H 5.56, N 14.86. Found: C 55.91, H 5.40, N 14.73.

5-[4-[4-(2,3-Dichlorophenyl)piperazin-1-yl]butoxy]pyrazolo[1,5-a]pyridine-2-carbaldehyde Oxime (8c). Compound 8c was prepared according to the protocol of 8a/b, using a solution of 7f (55.9 mg, 0.13 mmol) in ethanol (6.4 mL) as well as hydroxylamine hydrochloride (17.4 mg, 0.25 mmol) in H_2O (0.74 mL) and 2 M NaOH (0.07 mL, 0.14 mmol). Purification by flash chromatography (CH_2Cl_2 + 2% MeOH) yielded 8c as a white solid mixture of two isomers (47.9 mg, 82%, 3:1 ratio). Mp: 126 °C. IR (NaCl): 3855, 2950, 2819, 1647, 1577, 1448, 1242, 1205, 1138, 961 cm^{-1} . 1H NMR (DMSO- d_6 , 600 MHz): δ isomer 1 (75%) 1.59–1.66 (m, 2 H), 1.76–1.83 (m, 2 H), 2.41 (t, J = 7.2 Hz, 2 H), 2.52–2.59 (m, 4 H), 2.94–3.03 (m, 4 H), 4.06 (t, J = 5.9 Hz, 2 H), 6.56 (s, 1 H), 6.57 (dd, J = 7.9, 3.0 Hz, 1 H), 7.01 (d, J = 2.3 Hz, 1 H), 7.12 (dd, J = 6.5, 3.1 Hz, 1 H), 7.28–7.32 (m, 2 H), 8.13 (s, 1 H), 8.48 (ddd, J = 7.4, 0.3, 0.3 Hz, 1 H), 11.42 (s, 1 H); isomer 2 (25%) 1.59–1.66 (m, 2 H), 1.76–1.83 (m, 2 H), 2.41 (t, J = 7.2 Hz, 2 H), 2.52–2.59 (m, 4 H), 2.94–3.03 (m, 4 H), 4.06 (t, J = 5.9 Hz, 2 H), 6.64 (dd, J = 7.6, 2.6 Hz, 1 H), 7.06 (d, J = 0.8 Hz, 1 H), 7.08 (d, J = 2.3 Hz, 1 H), 7.12 (dd, J = 6.5, 3.1 Hz, 1 H), 7.28–7.32 (m, 2 H), 7.57 (s, 1 H), 8.52 (ddd, J = 7.3, 0.3, 0.3 Hz, 1 H), 11.74 (s, 1 H). ^{13}C NMR (DMSO- d_6 , 600 MHz): δ isomer 1 (75%) 22.6, 26.2, 51.0, 52.8, 57.2, 67.9, 92.2, 95.6, 107.2, 119.5, 124.3, 126.0, 128.4, 129.4, 132.6, 141.7, 142.6, 148.6, 151.2, 155.5; isomer 2 (25%) 22.6, 26.2, 51.0, 52.8, 57.2, 67.9, 96.1, 99.2, 108.2, 119.5, 124.3, 126.0, 128.4, 129.6, 132.6, 139.6, 141.3, 144.9, 151.2, 155.1. HPLC: t_R = 16.3 min, purity 97%. HR-EIMS: calcd 461.1385; found 461.1386.

5-[4-[4-(2,3-Dichlorophenyl)piperazin-1-yl]butoxy]pyrazolo[1,5-a]pyridine-3-carbonitrile (9a). A solution of 8a,b (126 mg, 0.27 mmol) in acetic anhydride (1.35 mL) was refluxed for 8 h. Then, ice-cold water was added, and after extraction with $CHCl_3$, the combined organic layers were dried over Na_2SO_4 . Purification by flash chromatography (CH_2Cl_2 + 2% MeOH) yielded 9a as an off-white solid (86.4 mg, 72%). Mp: 118 °C. IR (NaCl): 3065, 2948, 2817, 2219, 1648, 1578, 1542, 1243, 1064, 781 cm^{-1} . 1H NMR ($CDCl_3$, 600 MHz): δ 1.73–1.78 (m, 2 H), 1.90–1.95 (m, 2 H), 2.53 (t, J = 7.6 Hz, 2 H), 2.67–2.72 (m, 4 H), 3.07–3.12 (m, 4 H), 4.11 (t, J = 6.4 Hz, 2 H), 6.66 (d, J = 7.6 Hz, 1 H), 6.94 (d, J = 2.6 Hz, 1 H), 7.13–7.17 (m, 2 H), 8.11 (s, 1 H), 8.35 (d, J = 7.6, 1 H). ^{13}C NMR ($CDCl_3$, 600 MHz): δ 23.2, 26.8, 51.3, 53.3, 58.0, 68.9, 80.9, 95.0, 109.3, 114.5, 118.6, 124.7, 127.4, 127.5, 130.5, 134.0, 144.4, 145.6, 151.2, 159.2. HPLC: t_R = 18.8 min, purity 100%. APCI-MS: m/z 444 [M^+], 446 [$M^+ + 2$].

5-[4-[4-(2,3-Dichlorophenyl)piperazin-1-yl]butoxy]pyrazolo[1,5-a]pyridine-2-carbonitrile (9b). Cyanuric chloride (25.1 mg, 0.136 mmol) was dissolved in DMF (0.54 mL) under ice cooling. After 5 min at 0 °C the mixture was warmed to room temperature and stirred for 45 min. The formed suspension was subsequently added dropwise to a solution of 8c (63.1 mg, 0.136 mmol) in DMF (2.0 mL). After stirring at room temperature for 7 h, saturated $NaHCO_3$ solution was added and the aqueous layer was extracted with $CHCl_3$. The combined organic layers were dried over $MgSO_4$ and concentrated. The residue was purified by flash chromatography (CH_2Cl_2 + 0.5% MeOH) to give 9b as white solid (39.3 mg, 65%). Mp: 128 °C. IR (NaCl): 3090, 2942, 2874, 2813, 2236, 1649, 1577, 1448, 1428, 1378, 1239, 1209, 1134 cm^{-1} . 1H NMR ($CDCl_3$, 600 MHz): δ 1.70–1.77 (m, 2 H), 1.87–1.94 (m, 2 H), 2.51 (t, J = 7.6 Hz, 2 H), 2.62–2.70 (m, 4 H), 3.04–3.13 (m, 4 H), 4.04 (t, J = 6.3 Hz, 2 H), 6.66 (dd, J = 7.6, 2.6 Hz, 1 H), 6.71 (d, J = 0.8 Hz, 1 H), 6.76 (d, J = 2.6 Hz, 1 H), 6.95 (dd, J = 7.3, 2.2 Hz, 1 H), 7.13–7.17 (m, 2 H), 8.29 (ddd, J = 7.6, 0.4, 0.4 Hz, 1 H). ^{13}C NMR ($CDCl_3$, 360 MHz): δ 23.4, 26.8, 51.3, 53.3, 58.0, 68.4, 95.6, 101.2, 110.3, 114.3, 118.5, 124.6, 127.3, 127.4, 127.5, 129.4, 134.1, 141.5, 151.2, 156.7. HPLC: t_R = 17.0 min, purity 96%. HR-EIMS: calcd 443.1280; found 443.1280.

Receptor Binding Studies. Receptor binding studies were carried out as described previously.⁷⁶ Briefly, for competition binding experiments with the human D_{2L} , D_{2S} ,⁷⁷ D_3 ,⁷⁸ and $D_{4.4}$ ⁷⁹ receptors, preparations of membranes from CHO cells stably expressing the

corresponding receptor were used together with [3H]spiperone (specific activity of 81 Ci/mmol, Perkin-Elmer, Rodgau, Germany) at a final concentration of 0.10–0.30 nM. The assays were carried out at a protein concentration of 2–12 μg /assay tube, with observed K_D values of 30–85, 85–180, 30–95, and 130–290 pM and corresponding B_{max} values of 500–1600, 2200–6500, 2600–4800, and 580–2600 fmol/mg protein for the D_{2L} , D_{2S} , D_3 , and $D_{4.4}$ receptors, respectively. Competition binding experiments with the human D_1 ⁸⁰ and 5-HT_{2A}^{81,82} receptors were performed in an analogous manner with membranes from HEK 293 cells transiently transfected with these target receptors at a protein concentration of 3 and 4–6 μg /well, together with [3H]SCH23990 (specific activity 60 Ci/mmol, Biotrend, Cologne, Germany) (final concentration 0.40–0.50 nM, K_D = 0.32–0.48 nM, B_{max} = 3000 fmol/mg) or [3H]ketanserin (specific activity of 53 Ci/mmol, PerkinElmer, Rodgau, Germany) (final concentration 0.20–0.50 nM, K_D = 0.19–0.40 nM, B_{max} = 1000–2500 fmol/mg), respectively. Binding studies with the porcine dopamine D_1 , serotonin, and adrenergic receptors were carried out as described previously.⁷⁶ Homogenates from porcine striatum (D_1) or cerebral cortex were prepared, and assays were run with membranes at a protein concentration per each assay tube of 40, 80, 80, and 20–60 μg /mL for pD₁, p5-HT_{1A}, p5-HT₂, and p α_1 , respectively, in the presence of the radioligands [3H]SCH23990 (0.30 nM final concentration, K_D = 0.47–0.67 nM, B_{max} = 24–500 fmol/mg), [3H]WAY100635 (specific activity of 80 Ci/mmol, Biotrend, Cologne, Germany) (0.30 nM final concentration, K_D = 30–60 pM, B_{max} = 40–90 fmol/mg), [3H] ketanserin (0.50 nM final concentration, K_D = 1.1–2.2 nM, B_{max} = 120–520 fmol/mg), and [3H]prazosin (specific activity of 83 Ci/mmol, PerkinElmer, Rodgau, Germany) (0.10–0.20 nM final concentration, K_D = 40–87 pM, B_{max} = 80–340 fmol/mg), respectively. Competition binding experiments with V2.61F mutants of human D_{2L} and D_3 receptors were carried out as described previously²⁶ in the presence of [3H]spiperone (0.30 and 0.50 nM final concentration, protein concentration 10 and 50 μg /mL, K_D = 0.25 and 0.37 nM, B_{max} = 3400 and 1360 fmol/mg for hD_{2L}V2.61F and hD₃V2.61F, respectively). Protein concentration was determined by the method of Lowry using bovine serum albumin as standard.⁸³

Membrane Preparations of Transiently Transfected HEK 293 Cells. Membrane preparations were obtained using the methods described previously.⁸⁴ Briefly, HEK 293 cells were grown to a confluence of 70% and transiently transfected with the receptor of interest and a PTX-insensitive $G\alpha$ subunit using the Mirus TransIT-293 transfection reagent (purchased from MoBiTec, Goettingen, Germany) (for D_{2S} + $G\alpha_{i2}$ and D_3 + $G\alpha_{o1}$) or by $CaHPO_4$ precipitation method (for D_{2S} + $G\alpha_{o1}$); 48 h after transfection, cells were washed with ice-cold phosphate-buffered saline (PBS, pH 7.4) and detached by rinsing with harvest buffer (10 mM Tris-HCl, 0.5 mM EDTA, 5.4 mM KCl, 140 mM NaCl, pH 7.4). After centrifugation (8 min, 220g) the pellet was resuspended in 10 mL of ice cold homogenate buffer (50 mM Tris-HCl, 5 mM EDTA, 1.5 mM $CaCl_2$, 5 mM $MgCl_2$, 5 mM KCl, 120 mM NaCl, pH 7.4), and subsequently, cells were lysed with an Ultraturax. After ultracentrifugation at 50 000g the membranes were resuspended in binding buffer (50 mM Tris-HCl, 1 mM EDTA, 5 mM $MgCl_2$, 100 μg /mL bacitracin, 5 μg /mL soybean trypsin inhibitor, pH 7.4) and homogenized with a glass-Teflon homogenizer at 4 °C. Membrane preparations were shock-frozen in liquid nitrogen and stored at –80 °C until usage. The protein concentration was determined with the method of Lowry⁸³ applying bovine serum albumin as standard.

[^{35}S]GTP γ S Incorporation Assay. The [^{35}S]GTP γ S binding assay was performed on membrane preparations of transiently transfected HEK 293 cells expressing the corresponding dopamine receptor and a PTX-insensitive $G\alpha$ G-protein subunit (D_{2S} + $G\alpha_{o1}$, D_{2S} + $G\alpha_{i2}$, D_3 + $G\alpha_{o1}$). The receptor expression level was determined in saturation experiments with [3H]spiperone (1490 \pm 190, 4840 \pm 510, and 1150 \pm 140 fmol/mg protein, respectively). For control experiments, cells were treated with PTX (Calbiochem, 2.5 μL per culture dish) for 18 h prior to membrane preparation to inactivate endogenous G-proteins. The assay was carried out in 96-well plates with a final volume of 200

μL . In each well, 10 μM GDP, the compounds (from 0.1 pM to 10 μM final concentration, for quinpirole up to 1 mM), and the membranes (30 $\mu\text{g}/\text{mL}$ final protein concentration) were incubated for 30 min at 37 °C in incubation buffer containing 20 mM HEPES, 10 mM $\text{MgCl}_2 \cdot 6\text{H}_2\text{O}$, 100 mM NMDG, and 70 mg/L saponin.^{85–87} After the addition of 0.1 nM [³⁵S]GTP γ S (specific activity 1250 Ci/mmol, PerkinElmer, Rodgau, Germany), incubation was continued for another 75 min at 37 °C (30 min for D_{25} + $G\alpha_{o1}$). The equilibration was terminated by filtration through Whatman GF/B filters soaked with ice-cold PBS. Bound radioactivity was measured as described previously.⁸⁴ Four to six experiments per compound were performed with each concentration in triplicate.

β -Arrestin-2 Recruitment Assay. The measurement of receptor stimulated β -arrestin-2 recruitment was performed using the PathHunter assay (DiscoveRx, Birmingham, U.K.) according to the manufacturer's protocol. In brief, HEK-293 cells stably expressing the enzyme acceptor (EA) tagged β -arrestin-2 fusion protein were grown to a confluence of approximately 70% and transiently transfected with the ProLink tagged D_{25} -ARMS2PK2 construct by applying TransIT-293 Mirus transfection reagent (MoBiTec, Goettingen, Germany). Twenty-four hours after transfection, cells were detached from the culture dish with Versene (Life Technologies GmbH, Darmstadt, Germany), seeded into 384-well plates (5000 cells/well), and maintained for 24 h at 37 °C. After incubation with the test compounds dissolved in PBS (10 μM or for dose–response curves 1 pM up to 10 μM final concentration) for 6 h at 37 °C the detection mix was added and incubation was continued for a further 60 min at room temperature. Chemiluminescence was determined using the Victor³-V plate reader (Perkin-Elmer, Rodgau, Germany). For the inhibition experiments, cells were treated in an analogous manner and incubated with the test compounds dissolved in PBS (1 pM to 100 μM final concentration) together with quinpirole (100 nM final concentration). Three to eight experiments per compound were performed, with each concentration at least in duplicate.

Data Analysis. The resulting competition curves of the receptor binding experiments were analyzed by nonlinear regression using the algorithms in PRISM 5.0 (GraphPad software, San Diego, CA). The data were initially fit using a sigmoid model to provide an IC_{50} value representing the concentration corresponding to 50% of maximal inhibition. IC_{50} values were transformed to K_i values according to the equation of Cheng and Prusoff.⁸⁸ Dose–response curves of [³⁵S]GTP γ S binding were analyzed by nonlinear regression using the algorithms in PRISM 6.0 (GraphPad software, San Diego, CA), fitted with a sigmoid model and normalized to basal binding of radioactivity (0%) and the maximal effect caused by the reference full agonist quinpirole (100%). For each dose–response curve, a pEC_{50} value representing the concentration corresponding to 50% of maximal radioactive binding (E_{max}) was calculated. Dose–response curves of β -arrestin-2 recruitment were analyzed in the same way as [³⁵S]GTP γ S binding curves, normalizing to basal luminescence (0%) and the maximal luminescence caused by quinpirole (100%). Dose–response curves of the inhibition of β -arrestin-2 recruitment were analyzed in an analogous manner and normalized to the maximal effect of 100 nM quinpirole (100%) and the maximal inhibition caused by 10 μM haloperidol (0%). The operational model of agonism⁶⁰ was used to quantify ligand bias as described previously.¹³ In brief, dose–response curves for the agonists were fitted to the following equations by applying the algorithms of PRISM 6.0

$$Y = \text{basal} + \frac{E_m - \text{basal}}{1 + 10^{(\log \text{EC}_{50} - \log [X])}}$$

with basal being the response of a the system in the absence of an agonist, E_m the maximal response, EC_{50} the concentration necessary to obtain a half-maximal effect, and $[X]$ the concentration of the agonist. Transduction coefficients (τ/K_A) were used to quantify the ligand bias along different signaling pathways and obtained in their logarithmic form from

$$Y = \text{basal} + \frac{(E_m - \text{basal}) \left(\frac{\tau}{K_A} \right)^n [X]^n}{\left(\frac{\tau}{K_A} \right)^n [X]^n + \left(1 + \frac{[X]}{K_A} \right)^n}$$

where K_A is the equilibrium dissociation constant of the compound (X), τ the transducer constant, and n the transducer slope. As Hill slopes were close to unity, this parameter was fixed to 1.0 throughout the analysis. Transduction coefficients were then normalized to the response of the endogenous agonist dopamine to account for cell-system-dependent factors between different assay systems.

$$\Delta \log \left(\frac{\tau}{K_A} \right) = \log \left(\frac{\tau}{K_A} \right)_{\text{partial agonist}} - \log \left(\frac{\tau}{K_A} \right)_{\text{dopamine}}$$

Final quantification was performed by comparison of $\Delta \Delta \log(\tau/K_A)$ between different signaling pathways for D_{25} receptors or between D_{25} and D_3 receptors for signaling via $G\alpha_{o1}$.

Experimental Procedures for in Vivo Studies in Mice.

Assessment of the startle response for compound **7a** was performed by PsychoGenics Inc., Tarrytown, NY. All animals were handled in accordance to the guidelines defined by the institutional Animal Care and Use Committee. Adult, male C57Bl/6J mice were housed in groups of four on a 12 h light/dark cycle (light on at 7:00) with food and water ad libitum. Whole-body startles were measured in a sound-proofed chamber. Compound **7a** was dissolved in 1% Lutrol, 0.5% carboxymethylcellulose in 50 mM citrate buffer and administered ip 15 min before the measurement (3 mg/kg). After a period of habituation (5 min) to white noise background (70 dB), the startle pulse (120 dB, 40 ms) was delivered to measure the animal's startle response.

Molecular Docking. The investigated test compounds **7a** and **8b** were geometry-optimized by means of Gaussian 09⁸⁹ at the HF/6-31(d,p) level (attributing a formal charge of +1). We docked these compounds into a recently published D_2 model¹⁷ (compound **8b**) and the crystal structure of the D_3 receptor⁶⁸ (compound **7a**) using AutoDock Vina⁹⁰ as previously described.¹⁷ On the basis of the scoring function of AutoDock Vina and experimental data, we selected one conformation of compound **8b** in D_2 and four conformations of compound **7a** in D_3 (Figure S3, Supporting Information). Each ligand–receptor complex was submitted to an energy minimization procedure as described.¹⁷

Docking Refinement. To select one conformation of compound **7a** in D_3 for subsequent membrane simulations, we performed molecular dynamics simulation runs of 30 ns in a water box at 310 K on each of the four minimized **7a**– D_3 complexes using Amber10.⁹¹ The all-atom force field ff99SB⁹² and the general Amber force field (GAFF)⁹³ were used for D_3 and compound **7a**, respectively. Parameters for the test compound were assigned using antechamber⁹¹ and charges were calculated using Gaussian 09 at the HF/6-31(d,p) level and the RESP procedure according to the literature.⁹⁴ A formal charge of +1 was defined for compound **7a**. The simulation steps were carried out in an octahedral TIP3P⁹⁵ water box with constant-pressure periodic boundary conditions. The SHAKE⁹⁶ algorithm was used to constrain bonds involving hydrogen atoms, thereby enabling an integration step size of 2 fs. The particle mesh Ewald (PME) method⁹⁷ was used to treat long-range electrostatics. The minimized complexes were gradually heated to 310 K over a simulation time of 500 ps by coupling to a temperature bath⁹⁸ and further equilibrated for 4.5 ns. During this procedure, initial restraints of 5.0 kcal mol⁻¹ Å⁻² were applied on the main chain atoms of the receptors, which were reduced to 0.5 kcal mol⁻¹ Å⁻² in a stepwise manner and maintained for the 30 ns simulation runs. Data were collected every picosecond and analyzed by means of the PTRAJ module of Amber10. Calculation of the binding free energies was accomplished using MMPBSA.py,⁹⁹ employing intervals of 1 ns between the snapshots. On the basis of these calculations, we selected one **7a**– D_3 complex for subsequent membrane simulations (Figure S4, Supporting Information). The final complex was submitted to an energy minimization procedure as described.¹⁷ Additionally, an identical MD-procedure was performed for the docked **8b**– D_2 complex.

Membrane Simulations. The Amber parameter topology and coordinate files for the MD-refined and minimized complexes (**7a** in D_3 and **8b** in D_2) were converted into GROMACS input files.^{100,101} Each ligand–receptor complex was inserted into a pre-equilibrated system bearing a hydrated membrane of dioleoylphosphatidylcholine (DOPC) lipids by means of the GROMACS tool *g_membed*.¹⁰² The membrane was built up according to a procedure successfully applied earlier¹⁰³ and equilibrated for 10 ns. The charges of the simulation systems were neutralized by adding 8 and 10 chlorine atoms to the **7a**– D_3 and the **8b**– D_2 complexes, respectively. In total, the **7a**– D_3 system consisted of 101 177 atoms (273 amino acids, 243 DOPC lipids, 21 090 water molecules), and the **8b**– D_2 system of 100 967 atoms (267 amino acids, 241 DOPC lipids, 21 090 water molecules). For the membrane simulations, GAFF was used for the ligands and the DOPC molecules and the force field ff99SB for the protein residues. The SPC/E water model¹⁰⁴ was applied. After insertion into the membrane, the simulation systems were submitted to a short simulation run of 10 ns each, with restraints of 1.0 kcal mol⁻¹ Å⁻² applied on the main chain atoms of D_2 and D_3 , and subsequent production molecular dynamics simulation runs of 200 and 100 ns for the **7a**– D_3 and **8b**– D_2 complexes, respectively, using the GROMACS 4.5.2 simulation package as described earlier.¹⁰³ The analysis of the trajectories was performed with the PTRAJ module of Amber10, and figures were prepared using PyMOL.¹⁰⁵

■ ASSOCIATED CONTENT

Supporting Information

Experimental data, NMR spectra, sequence alignments of DRD2 and DRD3, results of functional assays, calculations, and in vivo data. This material is available free of charge via the Internet at <http://pubs.acs.org>.

■ AUTHOR INFORMATION

Corresponding Author

*Phone: +49 9131 85-29383. Fax: +49 9131 85-22585. E-mail: peter.gmeiner@fau.de.

Notes

The authors declare no competing financial interest.

■ ACKNOWLEDGMENTS

The German Science Foundation (DFG) is acknowledged for financial support (GRK 1910). We thank Dr. Stefan Schuster and Dr. Nuska Tschammer for helpful discussions. We thank Prof. Graeme Milligan (University of Glasgow, U.K.) for providing us with the cDNA for $G\alpha_{o1}$ and $G\alpha_{i2}$ proteins, and we thank Dr. Nuska Tschammer and Tamara Schellhorn for the construction of the ARMS2-PK2-tagged D_{2S} receptor cDNA.

■ ABBREVIATIONS USED

aripiprazole, 7-[4-[4-(2,3-dichlorophenyl)piperazin-1-yl]butoxy]-3,4-dihydroquinolin-2(1H)-one; D_x , dopamine D_x receptor; GTP γ S, guanosine 5'-O-(thiotriphosphate); spiperone, 8-[4-(4-fluorophenyl)-4-oxobutyl]-1-phenyl-1,3,8-triazaspiro[4.5]decan-4-one; CHO, chinese hamster ovary; CNS, central nervous system; SEM, standard error of the mean; ketanserin, 3-[2-[4-(4-fluorobenzoyl)piperidin-1-yl]ethyl]quinazoline-2,4(1H,3H)-dione; prazosin, 2-[4-(2-furoyl)piperazin-1-yl]-6,7-dimethoxyquinazolin-4-amine; PTX, pertussis toxin; quinpirole, (4aR-trans)-4,4a,5,6,7,8,8a,9-octahydro-5-propyl-1H-pyrazolo[3,4-g]quinoline; APCI, atmospheric pressure chemical ionization; ESI, electrospray ionization; haloperidol, 4-(4-(4-chlorophenyl)-4-hydroxypiperidin-1-yl)-1-(4-fluorophenyl)butan-1-one; HEK, human embryonic kidney; bifeprunox, 7-[4-(biphenyl-3-ylmethyl)piperazin-1-yl]-1,3-benzoxazol-2(3H)-one; EPS, extrapyramidal side effects; 1,4-DAP,

1,4-disubstituted-aromatic piperazine; EL, extracellular loop; TM, transmembrane helix.

■ REFERENCES

- (1) Freedman, R. Schizophrenia. *New Engl. J. Med.* **2003**, *349*, 1738–1749.
- (2) Mailman, R. B.; Murthy, V. Third Generation Antipsychotic Drugs: Partial Agonism or Receptor Functional Selectivity? *Curr. Pharm. Des.* **2010**, *16*, 488–501.
- (3) DeLeon, A.; Patel, N. C.; Crismon, M. L. Aripiprazole: A Comprehensive Review of Its Pharmacology, Clinical Efficacy, and Tolerability. *Clin. Ther.* **2004**, *26*, 649–666.
- (4) Tadori, Y.; Kitagawa, H.; Forbes, R. A.; McQuade, R. D.; Stark, A.; Kikuchi, T. Differences in Agonist/Antagonist Properties at Human Dopamine D(2) Receptors between Aripiprazole, Bifeprunox and Sdz 208–912. *Eur. J. Pharmacol.* **2007**, *574*, 103–111.
- (5) Tadori, Y.; Forbes, R. A.; McQuade, R. D.; Kikuchi, T. Characterization of Aripiprazole Partial Agonist Activity at Human Dopamine D3 Receptors. *Eur. J. Pharmacol.* **2008**, *597*, 27–33.
- (6) Tadori, Y.; Miwa, T.; Tottori, K.; Burris, K. D.; Stark, A.; Mori, T.; Kikuchi, T. Aripiprazole's Low Intrinsic Activities at Human Dopamine D2L and D2S Receptors Render It a Unique Antipsychotic. *Eur. J. Pharmacol.* **2005**, *515*, 10–19.
- (7) Kiss, B.; Horvath, A.; Nemethy, Z.; Schmidt, E.; Laszlovszky, I.; Bugovics, G.; Fazekas, K.; Hornok, K.; Orosz, S.; Gyertyan, I.; Agai-Csongor, E.; Domany, G.; Tihanyi, K.; Adham, N.; Szombathelyi, Z. Cariprazine (Rgh-188), a Dopamine D(3) Receptor-Preferring, D(3)/D(2) Dopamine Receptor Antagonist-Partial Agonist Antipsychotic Candidate: In Vitro and Neurochemical Profile. *J. Pharmacol. Exp. Ther.* **2010**, *333*, 328–340.
- (8) Urban, J. D.; Clarke, W. P.; von Zastrow, M.; Nichols, D. E.; Kobilka, B.; Weinstein, H.; Javitch, J. A.; Roth, B. L.; Christopoulos, A.; Sexton, P. M.; Miller, K. J.; Spedding, M.; Mailman, R. B. Functional Selectivity and Classical Concepts of Quantitative Pharmacology. *J. Pharmacol. Exp. Ther.* **2007**, *320*, 1–13.
- (9) Rajagopal, K.; Lefkowitz, R. J.; Rockman, H. A. When 7 Transmembrane Receptors Are Not G Protein-Coupled Receptors. *J. Clin. Invest.* **2005**, *115*, 2971–2974.
- (10) Neve, K. A. *Functional Selectivity of G Protein-Coupled Receptor Ligands—New Opportunities for Drug Discovery*, 1st ed.; Humana Press: Totowa, NJ, 2009; pp 25–40.
- (11) Lefkowitz, R. J.; Shenoy, S. K. Transduction of Receptor Signals by Beta-Arrestins. *Science* **2005**, *308*, 512–517.
- (12) Wei, H.; Ahn, S.; Shenoy, S. K.; Karnik, S. S.; Hunyady, L.; Luttrell, L. M.; Lefkowitz, R. J. Independent Beta-Arrestin 2 and G Protein-Mediated Pathways for Angiotensin II Activation of Extracellular Signal-Regulated Kinases 1 and 2. *Proc. Natl. Acad. Sci. U. S. A.* **2003**, *100*, 10782–10787.
- (13) Shonberg, J.; Herenbrink, C. K.; Lopez, L.; Christopoulos, A.; Scammells, P. J.; Capuano, B.; Lane, J. R. A Structure–Activity Analysis of Biased Agonism at the Dopamine D2 Receptor. *J. Med. Chem.* **2013**, *56*, 9199–9221.
- (14) Allen, J. A.; Yost, J. M.; Setola, V.; Chen, X.; Sassano, M. F.; Chen, M.; Peterson, S.; Yadav, P. N.; Huang, X. P.; Feng, B.; Jensen, N. H.; Che, X.; Bai, X.; Frye, S. V.; Wetsel, W. C.; Caron, M. G.; Javitch, J. A.; Roth, B. L.; Jin, J. Discovery of Beta-Arrestin-Biased Dopamine D2 Ligands for Probing Signal Transduction Pathways Essential for Antipsychotic Efficacy. *Proc. Natl. Acad. Sci. U. S. A.* **2011**, *108*, 18488–18493.
- (15) Urban, J. D.; Vargas, G. A.; von Zastrow, M.; Mailman, R. B. Aripiprazole Has Functionally Selective Actions at Dopamine D2 Receptor-Mediated Signaling Pathways. *Neuropsychopharmacology* **2007**, *32*, 67–77.
- (16) Masri, B.; Salahpour, A.; Didriksen, M.; Ghisi, V.; Beaulieu, J. M.; Gainetdinov, R. R.; Caron, M. G. Antagonism of Dopamine D2 Receptor/Beta-Arrestin 2 Interaction Is a Common Property of Clinically Effective Antipsychotics. *Proc. Natl. Acad. Sci. U. S. A.* **2008**, *105*, 13656–13661.

- (17) Hiller, C.; Kling, R. C.; Heinemann, F. W.; Meyer, K.; Hubner, H.; Gmeiner, P. Functionally Selective Dopamine D2/D3 Receptor Agonists Comprising an Enyne Moiety. *J. Med. Chem.* **2013**, *56*, 5130–5141.
- (18) Bromberg, K. D.; Iyengar, R.; Cijiang He, J. Regulation of Neurite Outgrowth by $G_{i/o}$ Signaling Pathways. *Front. Biosci.* **2008**, *13*, 4544–4557.
- (19) Strittmatter, S. M.; Fishman, M. C.; Zhu, X. P. Activated Mutants of the Alpha Subunit of G(O) Promote an Increased Number of Neurites Per Cell. *J. Neurosci.* **1994**, *14*, 2327–2338.
- (20) Hwangpo, T. A.; Jordan, J. D.; Premisrirut, P. K.; Jayaraman, G.; Licht, J. D.; Iyengar, R.; Neves, S. R. G Protein-Regulated Inducer of Neurite Outgrowth (GRIN) Modulates Sprouty Protein Repression of Mitogen-Activated Protein Kinase (MAPK) Activation by Growth Factor Stimulation. *J. Biol. Chem.* **2012**, *287*, 13674–13685.
- (21) Nakata, H.; Kozasa, T. Functional Characterization of $G_{\alpha o}$ Signaling through G Protein-Regulated Inducer of Neurite Outgrowth I. *Mol. Pharmacol.* **2005**, *67*, 695–702.
- (22) Zimnisky, R.; Chang, G.; Gyertyan, I.; Kiss, B.; Adham, N.; Schmauss, C. Cariprazine, a Dopamine D(3)-Receptor-Preferring Partial Agonist, Blocks Phencyclidine-Induced Impairments of Working Memory, Attention Set-Shifting, and Recognition Memory in the Mouse. *Psychopharmacology* **2013**, *226*, 91–100.
- (23) Chen, X.; Sassano, M. F.; Zheng, L.; Setola, V.; Chen, M.; Bai, X.; Frye, S. V.; Wetsel, W. C.; Roth, B. L.; Jin, J. Structure-Functional Selectivity Relationship Studies of Beta-Arrestin-Biased Dopamine D(2) Receptor Agonists. *J. Med. Chem.* **2012**, *55*, 7141–7153.
- (24) Bettinetti, L.; Schlotter, K.; Hubner, H.; Gmeiner, P. Interactive SAR Studies: Rational Discovery of Super-Potent and Highly Selective Dopamine D3 Receptor Antagonists and Partial Agonists. *J. Med. Chem.* **2002**, *45*, 4594–4597.
- (25) Löber, S.; Hübner, H.; Utz, W.; Gmeiner, P. Rationally Based Efficacy Tuning of Selective Dopamine D4 Receptor Ligands Leading to the Complete Antagonist 2-[4-(4-Chlorophenyl)piperazin-1-ylmethyl]pyrazolo[1,5-*a*]pyridine (FAUC213). *J. Med. Chem.* **2001**, *44*, 2691–2694.
- (26) Ehrlich, K.; Gotz, A.; Bollinger, S.; Tschammer, N.; Bettinetti, L.; Harterich, S.; Hubner, H.; Lanig, H.; Gmeiner, P. Dopamine D2, D3, and D4 Selective Phenylpiperazines as Molecular Probes To Explore the Origins of Subtype Specific Receptor Binding. *J. Med. Chem.* **2009**, *52*, 4923–4935.
- (27) Gmeiner, P.; Sommer, J.; Mierau, J.; Hofner, G. Dopamine Autoreceptor Agonists—Computational Studies, Synthesis and Biological Investigations. *Bioorg. Med. Chem. Lett.* **1993**, *3*, 1477–1483.
- (28) Lober, S.; Aboul-Fadl, T.; Hubner, H.; Gmeiner, P. Di- and Trisubstituted Pyrazolo[1,5-*a*]pyridine Derivatives: Synthesis, Dopamine Receptor Binding and Ligand Efficacy. *Bioorg. Med. Chem. Lett.* **2002**, *12*, 633–636.
- (29) Gmeiner, P.; Huebner, H.; Skultety, M. Preparation of Indolizines and Aza-Analog Derivatives Thereof as CNS Active Compounds. WO 2008113559A2, 2008.
- (30) Huisgen, R.; Grashy, R.; Krischke, R. 1.3-Additionen Mit Pyridin-Imin, Chinolin-Imin, Isochinolin-Imin Und Phenanthridin-Imin. *Tetrahedron Lett.* **1962**, *3*, 387–391.
- (31) Kendall, J. D. Synthesis and Reactions of Pyrazolo[1,5-*a*]pyridines and Related Heterocycles. *Curr. Org. Chem.* **2011**, *15*, 2481–2518.
- (32) Loaiza, P. R.; Lober, S.; Hubner, H.; Gmeiner, P. Click Chemistry on Solid Phase: Parallel Synthesis of *N*-Benzyltriazole Carboxamides as Super-Potent G-Protein Coupled Receptor Ligands. *J. Comb. Chem.* **2006**, *8*, 252–261.
- (33) Lober, S.; Hubner, H.; Tschammer, N.; Gmeiner, P. Recent Advances in the Search for D3- and D4-Selective Drugs: Probes, Models and Candidates. *Trends Pharmacol. Sci.* **2011**, *32*, 148–157.
- (34) Oshiro, Y.; Sato, S.; Kurahashi, N.; Tanaka, T.; Kikuchi, T.; Tottori, K.; Uwahodo, Y.; Nishi, T. Novel Antipsychotic Agents with Dopamine Autoreceptor Agonist Properties: Synthesis and Pharmacology of 7-[4-(4-Phenyl-1-piperazinyl)butoxy]-3,4-dihydro-2(1*H*)-quinolinone Derivatives. *J. Med. Chem.* **1998**, *41*, 658–667.
- (35) Johnson, D. S.; Choi, C.; Fay, L. K.; Favor, D. A.; Repine, J. T.; White, A. D.; Akunne, H. C.; Fitzgerald, L.; Nicholls, K.; Snyder, B. J.; Whetzel, S. Z.; Zhang, L.; Serpa, K. A. Discovery of PF-00217830: Aryl Piperazine Naphthyridinones as D2 Partial Agonists for Schizophrenia and Bipolar Disorder. *Bioorg. Med. Chem. Lett.* **2011**, *21*, 2621–2625.
- (36) Vangveravong, S.; Zhang, Z.; Taylor, M.; Bearden, M.; Xu, J.; Cui, J.; Wang, W.; Luedtke, R. R.; Mach, R. H. Synthesis and Characterization of Selective Dopamine D(2) Receptor Ligands Using Aripiprazole as the Lead Compound. *Bioorg. Med. Chem.* **2011**, *19*, 3502–3511.
- (37) Ochi, H.; Miyasaka, T.; Kanada, K.; Arakawa, K. Studies of Heterocyclic Compounds. VIII. Synthesis and Tautomerism of 2-Hydroxypyrazolo[1,5-*a*]pyridine. *Bull. Chem. Soc. Jpn.* **1976**, *49*, 1980–1984.
- (38) Elsner, J.; Boeckler, F.; Davidson, K.; Sugden, D.; Gmeiner, P. Bicyclic Melatonin Receptor Agonists Containing a Ring-Junction Nitrogen: Synthesis, Biological Evaluation, and Molecular Modeling of the Putative Bioactive Conformation. *Bioorg. Med. Chem.* **2006**, *14*, 1949–1958.
- (39) Brown, R. F. C.; Eastwood, F. W.; Fallon, G. D.; Lee, S. C.; Mcgeary, R. P. The Pyrolytic Rearrangement of 1-Alkynoyl-3-methylpyrazoles—Synthesis of Pyrazolo[1,5-*a*]pyridin-5-ols and Related-Compounds. *Aust. J. Chem.* **1994**, *47*, 991–1007.
- (40) Elsner, J.; Boeckler, F.; Heinemann, F. W.; Hubner, H.; Gmeiner, P. Pharmacophore-Guided Drug Discovery Investigations Leading to Bioactive 5-Aminotetrahydropyrazolopyridines. Implications for the Binding Mode of Heterocyclic Dopamine D3 Receptor Agonists. *J. Med. Chem.* **2005**, *48*, 5771–5779.
- (41) Boeckler, F.; Ohnmacht, U.; Lehmann, T.; Utz, W.; Hübner, H.; Gmeiner, P. CoMFA and CoMSIA Investigations Revealing Novel Insights into the Binding Modes of Dopamine D3 Receptor Agonists. *J. Med. Chem.* **2005**, *48*, 2493–2508.
- (42) Tanji, K.; Sasahara, T.; Suzuki, J.; Higashino, T. Pyrazolopyridines. 1. Formylation and Acylation of Pyrazolo[1,5-*a*]pyridines. *Heterocycles* **1993**, *35*, 915–924.
- (43) Moffett, R. B.; Hanze, A. R.; Seay, P. H. Central Nervous System Depressants. V. Polyhydroxy and Methoxyphenyl Ketones, Carbinols, and Derivatives. *J. Med. Chem.* **1964**, *7*, 178–186.
- (44) De Luca, L.; Giacomelli, G.; Porcheddu, A. Beckmann Rearrangement of Oximes under Very Mild Conditions. *J. Org. Chem.* **2002**, *67*, 6272–6274.
- (45) Dulcere, J. P. Vilsmeier Reagent for a High-Yield Conversion of Aldoximes to Nitriles. *Tetrahedron Lett.* **1981**, *22*, 1599–1600.
- (46) Sternweis, P. C.; Robshaw, J. D. Isolation of Two Proteins with High Affinity for Guanine Nucleotides from Membranes of Bovine Brain. *J. Biol. Chem.* **1984**, *259*, 13806–13813.
- (47) Lane, J. R.; Powney, B.; Wise, A.; Rees, S.; Milligan, G. G. Protein Coupling and Ligand Selectivity of the D2l and D3 Dopamine Receptors. *J. Pharmacol. Exp. Ther.* **2008**, *325*, 319–330.
- (48) Cordeaux, Y.; Nickolls, S. A.; Flood, L. A.; Graber, S. G.; Strange, P. G. Agonist Regulation of D2 Dopamine Receptor/G Protein Interaction: Evidence for Agonist Selection of G Protein Subtype. *J. Biol. Chem.* **2001**, *276*, 28667–28675.
- (49) Gazi, L.; Nickolls, S. A.; Strange, P. G. Functional Coupling of the Human Dopamine D2 Receptor with $G_{\alpha_{i1}}$, $G_{\alpha_{i2}}$, $G_{\alpha_{i3}}$, and G_{α_o} G Proteins: Evidence for Agonist Regulation of G Protein Selectivity. *Br. J. Pharmacol.* **2003**, *138*, 775–786.
- (50) Ahlgren-Beckendorf, J. A.; Levant, B. Signaling Mechanisms of the D3 Dopamine Receptor. *J. Recept. Signal Transduction* **2004**, *24*, 117–130.
- (51) Jiang, M.; Spicher, K.; Boulay, G.; Wang, Y.; Birnbaumer, L. Most Central Nervous System D2 Dopamine Receptors Are Coupled to Their Effectors by G_o . *Proc. Natl. Acad. Sci. U.S.A.* **2001**, *98*, 3577–3582.
- (52) Garey, L. J.; Ong, W. Y.; Patel, T. S.; Kanani, M.; Davis, A.; Mortimer, A. M.; Barnes, T. R.; Hirsch, S. R. Reduced Dendritic Spine Density on Cerebral Cortical Pyramidal Neurons in Schizophrenia. *J. Neurol. Neurosurg. Psychiatry* **1998**, *65*, 446–453.

- (53) Glantz, L. A.; Lewis, D. A. Decreased Dendritic Spine Density on Prefrontal Cortical Pyramidal Neurons in Schizophrenia. *Arch. Gen. Psychiatry* **2000**, *57*, 65–73.
- (54) Hill, J. J.; Hashimoto, T.; Lewis, D. A. Molecular Mechanisms Contributing to Dendritic Spine Alterations in the Prefrontal Cortex of Subjects with Schizophrenia. *Mol. Psychiatry* **2006**, *11*, 557–566.
- (55) Pauwels, P. J.; Tardif, S.; Wurch, T.; Colpaert, F. C. Facilitation of Constitutive A2a-Adrenoceptor Activity by Both Single Amino Acid Mutation (Thr373Lys) and *Gαo* Protein Coexpression: Evidence for Inverse Agonism. *J. Pharmacol. Exp. Ther.* **2000**, *292*, 654–663.
- (56) Asano, T.; Morishita, R.; Semba, R.; Itoh, H.; Kaziro, Y.; Kato, K. Identification of Lung Major Gtp-Binding Protein as Gi2 and Its Distribution in Various Rat-Tissues Determined by Immunoassay. *Biochemistry* **1989**, *28*, 4749–4754.
- (57) Valenzuela, D.; Han, X.; Mende, U.; Fankhauser, C.; Mashimo, H.; Huang, P.; Pfeiffer, J.; Neer, E. J.; Fishman, M. C. *Gαo* Is Necessary for Muscarinic Regulation of Ca²⁺ Channels in Mouse Heart. *Proc. Natl. Acad. Sci. U. S. A.* **1997**, *94*, 1727–1732.
- (58) Jiang, M.; Bajpayee, N. S. Molecular Mechanisms of Go Signaling. *Neurosignals* **2009**, *17*, 23–41.
- (59) Gardner, B. R.; Hall, D. A.; Strange, P. G. Agonist Action at D2(Short) Dopamine Receptors Determined in Ligand Binding and Functional Assays. *J. Neurochem.* **2002**, *69*, 2589–2598.
- (60) Black, J. W.; Leff, P. Operational Models of Pharmacological Agonism. *Proc. R. Soc. London, Ser. B* **1983**, *220*, 141–162.
- (61) Rajagopal, S.; Ahn, S.; Rominger, D. H.; Gowen-MacDonald, W.; Lam, C. M.; DeWire, S. M.; Violin, J. D.; Lefkowitz, R. J. Quantifying Ligand Bias at Seven-Transmembrane Receptors. *Mol. Pharmacol.* **2011**, *80*, 367–377.
- (62) Kenakin, T.; Watson, C.; Muniz-Medina, V.; Christopoulos, A.; Novick, S. A Simple Method for Quantifying Functional Selectivity and Agonist Bias. *ACS Chem. Neurosci.* **2012**, *3*, 193–203.
- (63) Tschammer, N.; Bollinger, S.; Kenakin, T.; Gmeiner, P. Histidine 6.55 Is a Major Determinant of Ligand-Biased Signaling in Dopamine D2L Receptor. *Mol. Pharmacol.* **2011**, *79*, 575–585.
- (64) Kenakin, T.; Miller, L. J. Seven Transmembrane Receptors as Shapeshifting Proteins: The Impact of Allosteric Modulation and Functional Selectivity on New Drug Discovery. *Pharmacol. Rev.* **2010**, *62*, 265–304.
- (65) Christopoulos, A.; Kenakin, T. G Protein-Coupled Receptor Allosterism and Complexing. *Pharmacol. Rev.* **2002**, *54*, 323–374.
- (66) Caccia, S.; Invernizzi, R. W.; Nobili, A.; Pasina, L. A New Generation of Antipsychotics: Pharmacology and Clinical Utility of Cariprazine in Schizophrenia. *Ther. Clin. Risk Manage.* **2013**, *9*, 319–328.
- (67) Boeckler, F.; Leng, A.; Mura, A.; Bettinetti, L.; Feldon, J.; Gmeiner, P.; Ferger, B. Attenuation of 1-Methyl-4-phenyl-1,2,3,6-tetrahydropyridine (MPTP) Neurotoxicity by the Novel Selective Dopamine D3-Receptor Partial Agonist Fauc 329 Predominantly in the Nucleus Accumbens of Mice. *Biochem. Pharmacol.* **2003**, *66*, 1025–1032.
- (68) Chien, E. Y.; Liu, W.; Zhao, Q.; Katritch, V.; Han, G. W.; Hanson, M. A.; Shi, L.; Newman, A. H.; Javitch, J. A.; Cherezov, V.; Stevens, R. C. Structure of the Human Dopamine D3 Receptor in Complex with a D2/D3 Selective Antagonist. *Science* **2010**, *330*, 1091–1095.
- (69) Luedtke, R. R.; Mishra, Y.; Wang, Q.; Griffin, S. A.; Bell-Horner, C.; Taylor, M.; Vangveravong, S.; Dillon, G. H.; Huang, R. Q.; Reichert, D. E.; Mach, R. H. Comparison of the Binding and Functional Properties of Two Structurally Different D2 Dopamine Receptor Subtype Selective Compounds. *ACS Chem. Neurosci.* **2012**, *3*, 1050–1062.
- (70) Newman, A. H.; Beuming, T.; Banala, A. K.; Donthamsetti, P.; Pongetti, K.; LaBounty, A.; Levy, B.; Cao, J.; Michino, M.; Luedtke, R. R.; Javitch, J. A.; Shi, L. Molecular Determinants of Selectivity and Efficacy at the Dopamine D3 Receptor. *J. Med. Chem.* **2012**, *55*, 6689–6699.
- (71) Michino, M.; Donthamsetti, P.; Beuming, T.; Banala, A.; Duan, L.; Roux, T.; Han, Y.; Trinquet, E.; Newman, A. H.; Javitch, J. A.; Shi, L. A Single Glycine in Extracellular Loop 1 Is the Critical Determinant for Pharmacological Specificity of Dopamine D2 and D3 Receptors. *Mol. Pharmacol.* **2013**, *84*, 854–864.
- (72) Rosenkilde, M. M.; Benced-Jensen, T.; Frimurer, T. M.; Schwartz, T. W. The Minor Binding Pocket: A Major Player in 7TM Receptor Activation. *Trends Pharmacol. Sci.* **2010**, *31*, 567–574.
- (73) Park, S. W.; Lee, C. H.; Cho, H. Y.; Seo, M. K.; Lee, J. G.; Lee, B. J.; Seol, W.; Kee, B. S.; Kim, Y. H. Effects of Antipsychotic Drugs on the Expression of Synaptic Proteins and Dendritic Outgrowth in Hippocampal Neuronal Cultures. *Synapse* **2013**, *67*, 224–234.
- (74) Pereira, A.; Zhang, B.; Malcolm, P.; Sugiharto-Winarno, A.; Sundram, S. Quetiapine and Aripiprazole Signal Differently to ERK, p90RSK and C-Fos in Mouse Frontal Cortex and Striatum: Role of the Egf Receptor. *BMC Neurosci.* **2014**, *15*, 30.
- (75) Ishima, T.; Iyo, M.; Hashimoto, K. Neurite Outgrowth Mediated by the Heat Shock Protein Hsp90alpha: A Novel Target for the Antipsychotic Drug Aripiprazole. *Trans. Psychiatry* **2012**, *2*, e170.
- (76) Hübner, H.; Haubmann, C.; Utz, W.; Gmeiner, P. Conjugated Enynes as Nonaromatic Catechol Bioisosteres: Synthesis, Binding Experiments, and Computational Studies of Novel Dopamine Receptor Agonists Recognizing Preferentially the D3 subtype. *J. Med. Chem.* **2000**, *43*, 756–762.
- (77) Hayes, G.; Biden, T. J.; Selbie, L. A.; Shine, J. Structural Subtypes of the Dopamine D2 Receptor Are Functionally Distinct: Expression of the Cloned D2A and D2B Subtypes in a Heterologous Cell Line. *Mol. Endocrinol.* **1992**, *6*, 920–926.
- (78) Sokoloff, P.; Giros, B.; Martres, M. P.; Bouthenet, M. L.; Schwartz, J. C. Molecular-Cloning and Characterization of a Novel Dopamine Receptor (D3) as a Target for Neuroleptics. *Nature* **1990**, *347*, 146–151.
- (79) Asghari, V.; Sanyal, S.; Buchwaldt, S.; Paterson, A.; Jovanovic, V.; Van Tol, H. H. Modulation of Intracellular Cyclic Amp Levels by Different Human Dopamine D4 Receptor Variants. *J. Neurochem.* **1995**, *65*, 1157–1165.
- (80) Keababian, J. W.; Calne, D. B. Multiple Receptors for Dopamine. *Nature* **1979**, *277*, 93–96.
- (81) McKenna, D. J.; Peroutka, S. J. Differentiation of 5-Hydroxytryptamine2 Receptor Subtypes Using ¹²⁵I-R(-)2,5-Dimethoxy-4-iodophenylisopropylamine and ³H-Ketanserin. *J. Neurosci.* **1989**, *9*, 3482–3490.
- (82) Pierce, P. A.; Peroutka, S. J. Evidence for Distinct 5-Hydroxytryptamine2 Binding Site Subtypes in Cortical Membrane Preparations. *J. Neurochem.* **1989**, *52*, 656–658.
- (83) Lowry, O. H.; Rosebrough, N. J.; Farr, A. L.; Randall, R. J. Protein Measurement with the Folin Phenol Reagent. *J. Biol. Chem.* **1951**, *193*, 265–275.
- (84) Tschammer, N.; Elsner, J.; Goetz, A.; Ehrlich, K.; Schuster, S.; Ruberg, M.; Kuhhorn, J.; Thompson, D.; Whistler, J.; Hubner, H.; Gmeiner, P. Highly Potent 5-Aminotetrahydropyrazolopyridines: Enantioselective Dopamine D3 Receptor Binding, Functional Selectivity, and Analysis of Receptor–Ligand Interactions. *J. Med. Chem.* **2011**, *54*, 2477–2491.
- (85) Cohen, F. R.; Lazareno, S.; Birdsall, N. J. The Effects of Saponin on the Binding and Functional Properties of the Human Adenosine A1 Receptor. *Br. J. Pharmacol.* **1996**, *117*, 1521–1529.
- (86) Lin, H.; Saisch, S. G.; Strange, P. G. Assays for Enhanced Activity of Low Efficacy Partial Agonists at the D(2) Dopamine Receptor. *Br. J. Pharmacol.* **2006**, *149*, 291–299.
- (87) Koener, B.; Focant, M. C.; Bosier, B.; Maloteaux, J. M.; Hermans, E. Increasing the Density of the D2l Receptor and Manipulating the Receptor Environment Are Required To Evidence the Partial Agonist Properties of Aripiprazole. *Prog. Neuro-Psychopharmacol. Biol. Psychiatry* **2012**, *36*, 60–70.
- (88) Yung-Chi, C.; Prusoff, W. H. Relationship between the Inhibition Constant (Ki) and the Concentration of Inhibitor Which Causes 50 Per Cent Inhibition (I50) of an Enzymatic Reaction. *Biochem. Pharmacol.* **1973**, *22*, 3099–3108.

- (89) Frisch, M. J.; Trucks, G. W.; Schlegel, H. B.; Scuseria, G. E.; Robb, M. A.; Cheeseman, J. R.; Scalmani, G.; Barone, V.; Mennucci, B.; Petersson, G. A.; Nakatsuji, H.; Caricato, M.; Li, X.; Hratchian, H. P.; Izmaylov, A. F.; Bloino, J.; Zheng, G.; Sonnenberg, J. L.; Hada, M.; Ehara, M.; Toyota, K.; Fukuda, R.; Hasegawa, J.; Ishida, M.; Nakajima, T.; Honda, Y.; Kitao, O.; Nakai, H.; Vreven, T.; Montgomery, J. A.; Peralta, J. E.; Ogliaro, F.; Bearpark, M.; Heyd, J. J.; Brothers, E.; Kudin, K. N.; Staroverov, V. N.; Kobayashi, R.; Normand, J.; Raghavachari, K.; Rendell, A.; Burant, J. C.; Iyengar, S. S.; Tomasi, J.; Cossi, M.; Rega, N.; Millam, J. M.; Klene, M.; Knox, J. E.; Cross, J. B.; Bakken, V.; Adamo, C.; Jaramillo, J.; Gomperts, R.; Stratmann, R. E.; Yazyev, O.; Austin, A. J.; Cammi, R.; Pomelli, C.; Ochterski, J. W.; Martin, R. L.; Morokuma, K.; Zakrzewski, V. G.; Voth, G. A.; Salvador, P.; Dannenberg, J. J.; Dapprich, S.; Daniels, A. D.; Farkas, Foresman, J. B.; Ortiz, J. V.; Cioslowski, J.; Fox, D. J. *Gaussian 09*, Revision B.01; Gaussian: Wallingford, CT, 2009.
- (90) Trott, O.; Olson, A. J. Autodock Vina: Improving the Speed and Accuracy of Docking with a New Scoring Function, Efficient Optimization, and Multithreading. *J. Comput. Chem.* **2010**, *31*, 455–461.
- (91) Case, D. A.; Darden, T. A.; Cheatham III, T. E.; Simmerling, C. L.; Wang, J.; Duke, R. E.; Luo, R.; Crowley, M.; Walker, R. C.; Zhang, W.; Merz, K. M.; Wang, B.; Hayik, S.; Roitberg, A.; Seabra, G.; Kolossváry, I.; Wong, K. F.; Paesani, F.; Vanicek, J.; Wu, X.; Brozell, S. R.; Steinbrecher, T.; Gohlke, H.; Yang, L.; Tan, C.; Mongan, J.; Hornak, V.; Cui, G.; Mathews, D. H.; Seetin, M. G.; Sagui, C.; Babin, V.; Kollman, P. A. *Amber10*; University of California: San Francisco, 2008.
- (92) Hornak, V.; Abel, R.; Okur, A.; Strockbine, B.; Roitberg, A.; Simmerling, C. Comparison of Multiple Amber Force Fields and Development of Improved Protein Backbone Parameters. *Proteins* **2006**, *65*, 712–725.
- (93) Wang, J.; Wolf, R. M.; Caldwell, J. W.; Kollman, P. A.; Case, D. A. Development and Testing of a General Amber Force Field. *J. Comput. Chem.* **2004**, *25*, 1157–1174.
- (94) Bayly, C. I.; Cieplak, P.; Cornell, W. D.; Kollman, P. A. A Well-Behaved Electrostatic Potential Based Method Using Charge Restraints for Deriving Atomic Charges: The RESP Model. *J. Phys. Chem.* **1993**, *97*, 10269–10280.
- (95) Jorgensen, W. L.; Chandrasekhar, J.; Madura, J. D.; Impey, R. W.; Klein, M. L. Comparison of Simple Potential Functions for Simulating Liquid Water. *J. Chem. Phys.* **1983**, *79*, 926–935.
- (96) Ryckaert, J.-P.; Ciccotti, G.; Berendsen, H. J. C. Numerical Integration of the Cartesian Equations of Motion of a System with Constraints: Molecular Dynamics of *n*-Alkanes. *J. Comput. Phys.* **1977**, *23*, 327–341.
- (97) Darden, T.; York, D.; Pedersen, L. Particle Mesh Ewald: An $N \cdot \log(N)$ Method for Ewald Sums in Large Systems. *J. Chem. Phys.* **1993**, *98*, 10089.
- (98) Berendsen, H. J. C.; Postma, J. P. M.; van Gunsteren, W. F.; DiNola, A.; Haak, J. R. Molecular Dynamics with Coupling to an External Bath. *J. Chem. Phys.* **1984**, *81*, 3684–3690.
- (99) Miller, B. R.; McGee, T. D.; Swails, J. M.; Homeyer, N.; Gohlke, H.; Roitberg, A. E. Mmpbsa.Py: An Efficient Program for End-State Free Energy Calculations. *J. Chem. Theory Comput.* **2012**, *8*, 3314–3321.
- (100) Van Der Spoel, D.; Lindahl, E.; Hess, B.; Groenhof, G.; Mark, A. E.; Berendsen, H. J. Gromacs: Fast, Flexible, and Free. *J. Comput. Chem.* **2005**, *26*, 1701–1718.
- (101) Hess, B.; Kutzner, C.; van der Spoel, D.; Lindahl, E. Gromacs 4: Algorithms for Highly Efficient, Load-Balanced, and Scalable Molecular Simulation. *J. Chem. Theory Comput.* **2008**, *4*, 435–447.
- (102) Wolf, M. G.; Hoefling, M.; Aponte-Santamaria, C.; Grubmüller, H.; Groenhof, G. G_Membed: Efficient Insertion of a Membrane Protein into an Equilibrated Lipid Bilayer with Minimal Perturbation. *J. Comput. Chem.* **2010**, *31*, 2169–2174.
- (103) Goetz, A.; Lanig, H.; Gmeiner, P.; Clark, T. Molecular Dynamics Simulations of the Effect of the G-Protein and Diffusible Ligands on the Beta2-Adrenergic Receptor. *J. Mol. Biol.* **2011**, *414*, 611–623.
- (104) Berendsen, H. J. C.; Grigera, J. R.; Straatsma, T. P. The Missing Term in Effective Pair Potentials. *J. Phys. Chem.* **1987**, *91*, 6269–6271.
- (105) *The Pymol Molecular Graphics System*, Version 1.3r1; Schrodinger, LLC, 2010.